

*Investigation of
An Alternative Technique to Measure
Fracture Toughness of Paper*

Derrick Malcolm Spencer Wanigaratne

Bachelor of Science (Honours)

University of Peradeniya, Sri Lanka

Master of Science

Monash University, Clayton

**This thesis is submitted in fulfilment of the requirements for the
Degree of Doctor of Philosophy**

**Australian Pulp and Paper Institute
Department of Chemical Engineering**



MONASH University

August 2004

Declaration

I hereby declare that this thesis contains no material, which has been accepted for the award of any other degree or diploma in any university. To the best of my knowledge and belief, it contains no material previously written or published by another person, except where due reference is made.

Signed: -----

Derrick Malcolm Spencer Wanigaratne

Date: -----

Summary

The primary aim of the thesis is to develop a method for the rapid measurement of fracture toughness. A success in a rapid method will give the opportunity for the paper manufacturing and converting industry to use the fracture toughness as a quality control measurement.

The major outcome of this research work is the successful development and establishment of a new cyclic loading fracture toughness technique, which could be used to fulfil the industry requirements. The fracture toughness estimated from this method, not only correlated well with Essential Work Fracture (EWF) technique but also required much less time and sample area to determine a single value than EWF method. Tests conducted on more than 40 samples comparing EWF and cyclic method are given in this thesis.

The cyclic technique was then used to examine the effect of refining levels and humidity on fracture toughness. These measurements would be very difficult to complete within the time frame of the thesis if we use the EWF method. The work on the effect of humidity and level of refining on fracture toughness suggested that cyclic fracture toughness technique could be very effective in the study of fracture mechanisms, separation of plastic work from total work consumed in the fracture and to obtain fundamental information on fracture.

In the study of the effect of humidity on fracture toughness, it was observed that the load-extension behaviour of the sample has changed with change in humidity. At low moisture content the samples showed a brittle behaviour and fractured at lower strain than in standard paper testing laboratory conditions. At high moisture content the peak load of the load-extension curve was reduced and the sample breaking strain was increased. This suggested that the extreme humidity conditions were detrimental for the

fracture toughness of the paper. The optimum fracture toughness was observed at moderate moisture contents.

As a part of the thesis, a new image analysis technique was also developed to investigate the plastic deformation field of a sample prepared in DENT geometry. It was found that this method could be utilized as a useful tool to obtain valuable information on the shape of the deformation field.

This thesis also examined the correlation between individual and combined tensile parameters with fracture toughness. It was found that amongst individual tensile parameters, tensile index had the best correlation with fracture toughness. This correlation was better for laboratory made paper than machine made sheets. When the tensile parameters were combined, a better correlation to the fracture toughness was observed with a combination of tensile index and extension at maximum load. Although there was a reasonable correlation between combined tensile parameters and fracture toughness for laboratory made paper, this correlation was not strong enough to conclude that only the measurements of tensile properties are sufficient to predict fracture toughness. This work further reiterated the requirement of a unique and rapid test method to measure fracture toughness.

The research work carried out for this thesis which lead to the development and validation of a new cyclic fracture toughness technique, the development of new imaging technique to characterise deformation field, the correlations obtained between tensile properties and the fracture toughness and the research work carried out to test some of the proposed models to predict fracture toughness and sheet failure strength, has contributed to the advancement and better understanding of sheet fracture toughness.

Acknowledgements

I would like to thank my supervisor Dr. Warren Batchelor for his guidance, comments, advice and great flexibility throughout the time as a PhD student. Thank you also to my co-supervisor Associate Professor Ian Parker for his continuous support.

Dr. Andrew Conn deserves special thanks for his help especially with Excel macro's, and statistics. Thanks also to Paul Girling for introducing me the paper testing apparatus at the initial stages of PhD. I would also like to thank Richard Markowski, Jihong He and David Kelly for their assistance with the experiments. Thank you to all the staff and colleagues at APPI for their continuous support.

Thanks also to staff at the CSIRO Division of Forestry and Forest products, especially Maureen McHenry and Dr. Geoff Irvine for allowing to use the laboratory facilities. I would also like to thank Dr. Ajit Ghosh (former Amcor Research & Technology) and Dr. Paul Kibbelwhite (Papro, New Zealand) for providing samples for this research work.

Thank you to the staff of the Chemical and Mechanical Engineering Departmental Workshop for allowing me to use the facilities and helping me whenever technical assistance was required. In that respect I would like thank, Paul Beardsley, Peter Froud, Roy Harrip, and Gamini Ganegoda and Andrew Moore for their assistance.

I would like to give very special thank to my wife Anne and children for their continuous love and patience thought out these years. Thank you to my parents for giving me much needed encouragement.

This work was conducted as a part of the research program for the CRC for Hardwood Fibre and Paper Science. Funding received from the Australian Federal Government under the Cooperative research program is gratefully acknowledged.

Table of Contents

<i>Declaration</i>	<i>ii</i>
<i>Summary</i>	<i>iii</i>
<i>Acknowledgements</i>	<i>v</i>
<i>Table of Contents</i>	<i>vi</i>
<i>List of Figures</i>	<i>ix</i>
<i>List of Tables</i>	<i>xii</i>
<i>Glossary</i>	<i>xiii</i>
<i>Publications and Conference Papers</i>	<i>xiv</i>
1 Introduction	1
2 Literature Review	5
2.1 Introduction	5
2.2 Paper structure	5
2.2.1 Wood fibres	6
2.2.2 Inter-fibre bonds	8
2.2.3 Visco-elastic effects.....	9
2.2.4 Effect of moisture	10
2.3 In-plane mechanical properties of paper	11
2.3.1 Tensile index	11
2.3.2 Elastic modulus	12
2.3.3 Tensile energy absorption (TEA).....	12
2.3.4 Stretch at break	12
2.3.5 Elastic-plastic behaviour	12
2.3.6 Yield stress	13
2.4 Paper runnability	13
2.5 Historical development in paper web runnability studies	17
2.5.1 Statistical data collection	17
2.5.2 Mathematical modelling	18
2.5.3 Pilot tests	19
2.6 Correlation of basic mechanical properties with runnability	19
2.7 Tear strength as a web break controlling parameter	20
2.7.1 Elmendorf tear strength	21
2.7.2 In-plane tear test	22
2.8 Application of fracture mechanics to predict sheet failure	24
2.8.1 Linear Elastic Fracture Mechanics (LEFM)	24
2.8.2 Application of LEFM to paper.....	30
2.9 Non-linear fracture mechanics	38
2.9.1 Fracture Process Zone (FPZ).....	38
2.9.2 Developments in non-linear fracture measurement techniques	39
2.9.3 The J Integral method	41
2.9.4 Liebowitz non-linear technique (LNT)	46
2.9.5 Application of Liebowitz and J-integral techniques	47
2.9.6 Essential work of fracture technique (EWF)	54
2.10 Theoretical models on fracture toughness	63
2.11 Concluding remarks	68

3	Testing materials, equipment and methods	69
3.1	Introduction	69
3.2	Laboratory made paper	69
3.2.1	<i>Pulps</i>	69
3.2.2	<i>Disintegration and refining</i>	71
3.2.3	<i>Formation of laboratory sheets</i>	73
3.2.4	<i>Wet pressing</i>	74
3.2.5	<i>Sheet drying and storage</i>	75
3.2.6	<i>Thickness measurements</i>	75
3.3	Commercial papers	76
3.4	DENT sample preparation	76
3.4.1	<i>Cutting die</i>	76
3.4.2	<i>Press</i>	79
3.5	Testing environment	80
3.5.1	<i>Standard conditioned test room</i>	80
3.5.2	<i>Humidity Generator and relative humidity measurements</i>	81
3.5.3	<i>Sample conditioning</i>	81
3.6	Measurements of mechanical properties of paper	82
3.6.1	<i>EWF Fracture toughness</i>	82
3.6.2	<i>Tensile measurements</i>	87
3.6.3	<i>Zero-span tensile strength</i>	87
3.6.4	<i>Concluding remarks</i>	88
4	Image Analysis of plastic deformation in the fracture of paper	89
4.1	Introduction	89
4.2	Samples, apparatus and the technique	90
4.3	Sample straining	93
4.4	Calibration	93
4.5	Plastic deformation measurements	95
4.5.1	<i>Critical loads and displacements for DENT samples</i>	95
4.5.2	<i>CD DENT test piece</i>	97
4.5.3	<i>MD DENT test piece</i>	100
4.6	Estimation of plastic work in “Reflex” copy paper (CD direction)	102
4.7	Discussion	105
4.8	Conclusions	108
5	Comparison of fracture toughness of paper with tensile properties	109
5.1	Introduction	109
4.6	Materials	110
5.3	Results and Discussion	111
5.3.1	<i>EWF Results</i>	111
5.3.2	<i>Tensile properties</i>	120
5.4	The correlation of FT and tensile parameters	121
5.5	FT and combination of tensile parameters	124
5.6	Conclusions	133
6	A new cyclic loading technique for measuring fracture toughness of paper ...	135
6.1	Introduction	135
6.2	Alternative approaches of developing a new technique	135
4.7	Cyclic loading technique for the measurement of sheet fracture toughness	136
6.3.1	<i>Test Method</i>	136
6.3.2	<i>Test conditions</i>	141
4.8	Comparison of essential fracture work estimated from EWF and cyclic-loading techniques	144
4.9	The effect of ligament length on cyclic fracture toughness	146
4.10	Discussion	150

4.11	Prediction of paper failure strength using fracture toughness	152
4.12	Conclusions	156
7	<i>Use of cyclic loading technique to examine the effect of fibre refining and humidity on fracture toughness of paper</i>	158
7.1.	Introduction	158
7.2.	Materials and method	158
7.3.	The effect of refining in FT	160
7.3.1.	<i>Refining and fibre properties</i>	160
7.3.2.	<i>Variations in load-extension curves with refining</i>	161
7.3.3.	The effect of refining on apparent density	166
7.3.4.	<i>FT against apparent density</i>	168
7.3.5.	<i>Post failure pull-out energy</i>	170
7.3.6.	<i>The variation of post-failure pullout energy with fracture toughness</i>	171
7.3.7.	<i>The variations in plastic work with refining</i>	172
7.3.8.	<i>Plastic work and fracture toughness</i>	173
7.4.	Discussion	174
7.5.	Concluding remarks	179
7.6.	Testing of Shallhorn model for prediction of Fracture toughness	179
7.6.1.	<i>Shallhorn Model</i>	180
7.6.2.	<i>Concluding remarks</i>	187
7.6	The effect of humidity in FT	187
7.6.1	<i>Background</i>	187
7.6.2	<i>Medium coarseness pinus radiata</i>	190
7.6.3	<i>Ultra-low coarseness pinus radiata</i>	196
7.6.4	<i>Discussion</i>	199
7.7	Conclusions	203
8.	<i>Conclusions and recommendations for further work</i>	204
8.1	Conclusions	204
8.2	Recommendations for further work	207
9	<i>Bibliography</i>	209
APPENDIX A:		215
APPENDIX B:		221
APPENDIX C:		223
APPENDIX D:		224

List of Figures

Figure 2.1	Cell wall structure of a typical soft wood	7
Figure 2.2	Stress (σ) and strain (ϵ) against time (t).....	10
Figure 2.3	A typical load-extension curve for paper.....	11
Figure 2.4	Load-extension behaviour of linear-elastic and elastic-plastic material.....	12
Figure 2.5a	Optical microscopic image of a shive	14
Figure 2.6	Number of web breaks as a function of web tension.	16
Figure 2.7	Break frequency versus combination of tensile parameters	20
Figure 2.8	Out-of plane tear test	21
Figure 2.9	Failure modes of a material	22
Figure 2.10	In-plane tear sample configuration	23
Figure 2.11	An infinite body with a crack.....	25
Figure 2.12 (a)	Surface energy and potential energy contribution	26
Figure 2.13	The stress distribution and crack-tip correction	28
Figure 2.14	σ_N/σ_{YS} against sample width (2b)	31
Figure 2.15	K_c/ρ against specimen width	32
Figure 2.16	Critical failure stress against initial crack length.....	33
Figure 2.17 (a)	Short wide tensile specimen.....	34
Figure 2.18	Comparison -critical strain energy release rate and work of fracture (R).....	35
Figure 2.19	Stress-strain curves obtained from short and stable crack growth	37
Figure 2.20	FPZ and outer plastic zone of an elastic material and elastic-plastic material.....	39
Figure 2.21	Load –displacement curve of a double-notched sample.	40
Figure 2.22	Scanned image of the fractured sample after a tear test	40
Figure 2.23	The integration path Γ for the determination of J for a 2-D body.....	41
Figure 2.24	Typical graphical analysis of multiple specimen method	43
Figure 2.25	Load-displacement diagram of a double notched specimen	45
Figure 2.26	Typical load-elongation curve for a centre notched specimen.....	46
Figure 2.27	Specific fracture toughness against crack length to width ratio.....	47
Figure 2.28	Centre notched test configuration used in the STFI J-integral method.....	51
Figure 2.29	Plot of $J_1^b (= J_1.t_1)$ against δ_0 for the center notched test piece	53
Figure 2.30	Schematic load-elongation curve of a DENT specimen.	55
Figure 2.31	w_f against ligament length (L)	58
Figure 2.32	Stress and elongation of a DENT sample near crack tip	60
Figure 2.33	w_e against specific fracture energy.	60
Figure 2.34	Comparison between EWF and the J_c for different samples.	61
Figure 2.35	Experimental plots of w_f against L for (a) sack paper and (b) filter paper	62
Figure 2.36	Two parallel fibres crossing the rupture line.	66
Figure 4.1	Experimental set-up for image capturing system.....	90
Figure 4.2.	Part of a DENT sample near a crack tip.	91
Figure 4.3.	A typical image showing 7 lines.....	92
Figure 4.4.	Inverted average gray scale plot for the image in Figure 4.3	93
Figure 4.5	Line-spacing variation of a CD tensile test piece of copy paper with time	94
Figure 4.6.	The average Load against Extension data for copy paper	95
Figure 4.7.	Line-spacing variation of DENT sample near the crack-tip.	96
Figure 4.8.	Variation of line spacing with image distance.....	97

Figure 4.9.	Strain (%) versus frame distance from ligament	98
Figure 4.10.	Illustration of strain profile around ligament of Reflex copy paper in CD.....	99
Figure 4.11.	Line-spacing variation with image distance (from ligament),	100
Figure 4.12.	Strain (%) versus image distance (from ligament)	101
Figure 4.13.	Stress versus strain of cyclically loaded tensile test piece.....	102
Figure 4.14.	Envelop of nine cycles of the load-extension curve	103
Figure 4.15.	Plastic strain (%) versus specific plastic work	104
Figure 4.16.	Variation of total average plastic work per unit volume	105
Figure 5.1.	Load –Extension curves obtained from Reflex copy (MD)	112
Figure 5.2(a).	w_f against ligament length (L) of “Reflex” copy paper (MD)	113
Figure 5.3.	w_f against L & respective linear fits to plaster liner.	114
Figure 5.4.	w_f against L data for sack kraft along MD and CD.	115
Figure 5.5.	w_f against L for high coarseness <i>pinus radiata</i>	116
Figure 5.6.	w_f against L data for unbeaten medium coarseness radiata pine	117
Figure 5.7.	w_f against L data for lightly and heavily pressed medium coarseness.....	117
Figure 5.8.	w_f against L for lightly and heavily pressed, heavily beaten <i>pinus radiata</i>	118
Figure 5.9.	w_f vs L for lightly beaten, lightly pressed ultra-low coarseness <i>pinus radiata</i> ...	119
Figure 5.10.	Fracture toughness against TEA index.....	121
Figure 5.11.	FT against tensile index for machine made and laboratory made samples	122
Figure 5.12.	FT against elastic modulus	123
Figure 5.13.	FT against $A(\text{Tensile Index})^B (\text{Elastic modulus})^C$	125
Figure 5.14.	Elastic modulus against $0.11 \times (\text{Tensile Index})$ for all the samples.	126
Figure 5.15.	FT versus $m(\text{Tensile Index})^n (\text{TEA})^o$	127
Figure 5.16.	FT versus $p(\text{TEA})^q (\text{Elastic Modulus})^r$	127
Figure 5.17.	Tensile index against $a(\text{TEA})^b$ for all the samples	129
Figure 5.18.	Elastic modulus against $c(\text{TEA})^d$ for all the samples	129
Figure 5.19.	FT against $i(\text{TI})^j (\text{extension at max. load})^k$	130
Figure 5.20.	βw_p against FT for all samples and for only laboratory made samples.	133
Figure 6.1.	Cyclic load-extension curve of a DENT sample ultra-low coarseness	137
Figure 6.2.	FT estimated from the EWF and by the cyclic loading technique	140
Figure 6.3.	Cyclic load-extension curves from 25 and 90 mm span specimens	142
Figure 6.4.	Cyclic fracture toughness measured at different sample gauge lengths	143
Figure 6.5.	Variation of stored elastic energy at fracture with sample gauge length	143
Figure 6.6.	Comparison of EWF and cyclic fracture toughness for 43 test specimens.....	145
Figure 6.7.	FT measured from EWF and cyclic method at different ligament lengths	147
Figure 6.8.	FT measured from EWF and cyclic technique for plaster liner-board (MD) ..	147
Figure 6.9.	FT measured from EWF and cyclic technique for plaster liner-board (CD) ...	149
Figure 6.10.	Failure stress against predicted apparent strength.....	153
Figure 6.11.	Failure stress against predicted apparent strength for (a) high coarseness radiata pine refined for 75 minutes (b) plaster linerboard tested in CD and (c) plaster liner in MD directions.	155
Figure 7.1.	Typical cyclic load-extension curve of an unbeaten high coarseness radiata ..	159
Figure 7.2(i).	Cyclic load-extension curves (a) high (b) medium (c) ultra-low	162
Figure 7.3 a.	In-situ optical images of the ligament.....	164
Figure 7.4.	Apparent density as a function of pulp refining time in a Valley beater.	167
Figure 7.5.	Cyclic FT against apparent density, ultra-low coarseness).....	169
Figure 7.6.	Post-failure pull-out energy against apparent density.....	171
Figure 7.7.	Ratio of (PE/FT) against apparent density of radiata pine.....	172
Figure 7.8.	Plastic work as a proportion of total work against apparent density.....	172
Figure 7.9.	Variation of plastic work and fracture toughness of radiata pine	173
Figure 7.10.	(a) fibres trapped between beater bars (b) a knot that pulled tight on a fibre ..	176
Figure 7.11.	Zero span tensile properties of radiata pine samples	183
Figure 7.12.	Tensile index of radiata pine samples as a function of apparent density	183
Figure 7.13.	T/T ₀ against apparent density of radiata pine	184
Figure 7.14.	Calculated FT against apparent density for radiata pine.....	185

Figure 7.15	Tensile failure curves for kraft sack paper (MD).....	188
Figure 7.16	Representative load extension curves of medium coarseness radiata pine	191
Figure 7.17	FT against moisture content (%) for medium coarseness radiata pine	192
Figure 7.18	Plastic work against moisture content for medium coarseness samples.	193
Figure 7.19	Variation of post failure pullout energy against MC%	194
Figure 7.20	Images of the fracture lines of medium coarseness	195
Figure 7.21	Representative load-extension curves obtained from ultra-low coarseness (a). unrefined (b). 15 minutes & (c). 25 minutes refined.....	196
Figure 7.22	FT against moisture content (%) of ultra-low coarseness samples	197
Figure 7.23	Plastic work against moisture content for ultra-low coarseness samples	198
Figure 7.24	Post failure pull-out energy against MC% of ultra-low coarseness samples ...	199
Figure A1.	Fracture toughness test using EWF method.....	215
Figure B1.	Typical cyclic load-extension curves.....	215
Figure B2.	Last cycles of cyclic load-extension curves.....	215
Figure D1	Comparison of EWF vs Cyclic for machine made papaer.....	215

List of Tables

Table 3.1	Details of the pulp fibre.....	70
Table 3.2	Basic properties of commercial samples.....	76
Table 3.3	Details of newsprint samples.....	76
Table 3.4	Results with and without guide rods in the FT rig.....	86
Table 5.1	Summary of tensile properties.....	121
Table 5.2	Correlation between FT and Tensile properties.....	133
Table 6.1	Comparison of time required for testing FT using different methods	157
Table 7.1	Maximum slope of 1 st cycles of cyclic load-extension	168
Table 7.2	Maximum ratios of T/T ₀	188
Table 7.3	Maximum slopes of medium coarseness samples (10% & 90%RH)	194
Table 7.4	Maximum slopes of Ultra-low coarseness samples (10% & 90%RH)	199
Table A1	EWF test results for 15 DENT samples.....	219
Table B1	Typical data for a cyclic test	221

Glossary

APPITA – Technical Association of the Australian and New Zealand Pulp and Paper Industry

CD – Cross machine Direction of the machine made paper

CSF – Canadian Standard Freeness, a drainage test of pulp used as a measure of the level of refining

EFW- Essential Work of Fracture, is a technique use to measure fracture toughness

FT – Fracture toughness

grammage – the mass per unit area of a paper sheet

handsheet – laboratory produced paper sheet

linerboard – paperboard manufactured for use as liner in corrugated board

LEFM- Linear Elastic Fracture Mechanics, a method that is used to examine fracture with the assumption that the material is linear elastic

MD – machine direction of the machine made paper

NSSC – Neutral Sulfite Semi Chemical cooking process

Pinus radiata (radiata pine) main planted production species in New Zealand and the principal softwood grown in the plantation forests of Australia

refining - a step in the papermaking process where mechanical work is done on the pulp to improve fibre properties

viscoelastic – a material that exhibits both elastic and viscous behaviour

wet pressing – a step in the papermaking process where the newly formed paper sheet is pressed in the wet state to remove water and consolidate the sheet

Publications and Conference Papers

Publications

Wanigaratne, D., Batchelor, W. and Parker, I., “Comparison of fracture toughness of paper with tensile properties”, *Appita Journal*, 55(5):369-374, 385 (2002).

Wanigaratne, D., Batchelor, W. and Parker, I. and Conn, A. “Image analysis of plastic deformation in the fracture of paper”, *Appita Journal*, 53(6):471-475 (2000).

Batchelor, W and Wanigaratne, D., “A new cyclic loading method for measuring sheet fracture toughness”, *International Journal of Fracture*, 123, 15-27 (2003)

Wanigaratne, D., and Batchelor, W., “*Effect of humidity and refining on fracture toughness of paper*” (to be published)

Conference papers

Wanigaratne, D., Batchelor, W. and Parker, I. and Conn, A. “Image analysis of plastic deformation in the fracture of paper” *53rd Appita Annual General Conference* Rotorua, New Zealand, pp 759-764 (1999).

Wanigaratne, D., Batchelor, W. and Parker, I., “Comparison of fracture toughness of paper with tensile properties”, *55rd Appita Annual General Conference* Hobart, Australia pp 229-235 (2001)

Batchelor, W. and Wanigaratne, D., “A new cyclic loading method for measuring paper fracture toughness”, Proceedings of “*Progress in paper physics*”, Syracuse, NY, USA, September, 2002

1 Introduction

Paper sheet fracture in manufacturing and converting operations has been the subject of much research in the past three decades. Sheet fracture mainly occurs due to defects in the form of shives (unseparated fibre bundles), edge cracks, metals, plastics and pin holes within the material. Paper sheets generally experience in-plane stresses in manufacturing or converting operations and these stresses can concentrate around defects, which can then act as cracks in paper webs. The propagation of cracks causes paper web failure.

Fracture toughness is a measure of the resistance of a material to the propagation of cracks and it is a fundamental mechanical property. Although fracture toughness is a vital material parameter used to estimate the crack resistance of paper, its measurement is not currently carried out in manufacturing or converting operations as a quality control test. This is mainly because the time required to determine a single fracture toughness value using existing techniques is far too long for it to be carried out in a typical quality control cycle. Instead, out-of plane Elmendorf tear tests are commonly used to determine the crack resistance or quantify the runnability of paper. This practice has been subject to criticism mainly because the failure mode of the Elmendorf tear test is different to the failure mode in most of the end use situations, where stresses are applied in the plane of the sheet. In addition, Elmendorf tear test shows that the tear resistance deteriorates with refining, which is a mechanical action carried out to improve bonding between fibres in a sheet, while it is well established that other mechanical properties such as elastic modulus and tensile strength actually improve with refining. Further, there is no statistically established connection between the out-of plane tear resistance and the web break frequency.

The knowledge of fracture mechanics is vital for accurate measurement of the fracture toughness of a material. It is important to know whether the material behaves as a linear elastic or elastic-plastic material and then to decide whether linear elastic fracture mechanics or non-linear fracture mechanics should apply to the material to measure

fracture toughness. Application of the incorrect theory could give inaccurate and unreliable values.

In previous studies, linear elastic fracture mechanics (LEFM) was applied directly to various types of paper (Seth and Page 1974). However, the application of LEFM was not generally successful because many papers can show significant plastic deformation under tensile stress.

A few non-linear fracture mechanics methods, such as the J-integral and energy methods such as Essential Work of Fracture (EWF) method (Uesaka 1983b; Seth, Robertson et al. 1993) have also been applied to paper. With either the J-integral or EWF methods, the fracture toughness should be an intrinsic property of the material and independent of specimen or crack geometry. However, it has been shown that in some situations the values obtained using the J-integral method are not completely independent of sample or crack geometry (Westerlind, Carlsson *et al.* 1991). Based on the J-integral method an instrument has been developed to measure fracture toughness of paper (Wellmar, Fellers *et al.* 1997). Although this method has shown some potential to measure fracture toughness as a quality control parameter, it requires measurement of both notched and unnotched samples and complex mathematical analysis before the fracture toughness is determined.

The Essential Work of Fracture (EWF) technique has the ability to separate essential and non-essential work involved in the fracture of a sample. This method uses the deep Double-Edge Notched Tension (DENT) geometry, which consists of notches, where fracture is initiated, cut either side of a central ligament. There are a number of pre-conditions that must be satisfied for a successful measurement of fracture toughness using the EWF technique. When compared with the single specimen J-integral technique, the EWF method requires a large number of samples of different sizes to be measured to determine a single fracture toughness value. This method consumes a significant amount of time and sample area and in some instances the assumptions underlying the EWF method are not always valid either (Tanaka, Otsuka *et al.* 1997; Yu and Karenlampi 1997).

In other fracture studies of paper, the fracture toughness values estimated from the J-integral and the EWF methods were compared (Karenlampi, Cichoracki *et al.* 1998) and there was good agreement between the fracture toughness estimated from these two methods for less tough papers. However, the agreement was poor for tough ductile papers and the J-integral method seemed to underestimate the fracture toughness. More recently Tryding (2001) attempted to characterise tensile fracture properties of paper using the cohesive crack approach. The cohesive crack approach has been used successfully in characterising fracture in brittle or quasi-brittle materials such as concrete, plastics and laminates. However, application of the cohesive crack approach has been confined to research applications because it often requires the use of a computer with a high capacity for numerical calculations, since the method generally is combined with finite elemental analysis. Furthermore, there have been a few theoretical models proposed for the fracture toughness of paper (Shallhorn 1994; Niskanen, Karenlampi *et al.* 1996). However, so far these models are not well tested.

It is apparent that none of the existing approaches is completely successful in the measurement of fracture toughness of paper as a quality control measurement. There is a clear need for a quick and accurate technique, which requires measurements at only one sample size for measuring the fracture toughness of paper.

It is clear from the studies carried out using non-linear fracture mechanics that the work consumed for plastic deformation in the area outside the fracture process zone is the key factor making fracture toughness measurements so complicated. Therefore, from an elementary viewpoint, obtaining more information on the plastic deformation field around a crack is vital. The time and effort required to determine fracture toughness could be reduced if the work in the outer plastic zone could be estimated or separated from the total work, without the necessity of making measurements at multiple ligament lengths. Infra-red thermography was previously used to study the shape and size of the outer plastic zone and detailed information on the formation of the outer plastic deformation field was obtained (Tanaka, Otsuka *et al.* 1997; Tanaka and Yamauchi 1997). However, quantitative analysis on the work consumed in the deformation field during fracture was not made.

Although the use of the J-integral technique has been thoroughly investigated (Yuhara and Kortschot 1993; Wellmar, Fellers et al. 1997; Wellmar 2000), few studies have investigated the use of the EWF method. Therefore, it appears that the EWF technique offers greater potential for providing a new technique to measure fracture toughness.

The main aim of this project is, therefore, to develop an alternative technique that can be used to measure sheet fracture toughness as a quality control measurement in manufacturing and other converting operations. The technique should be quick, accurate and be able to measure an intrinsic property of the material. This new technique should require measurements at only one sample size.

Another aim of the project is to investigate the relationship between in-plane fracture toughness and other tensile properties such as elastic modulus, tensile strength and tensile energy absorption (TEA) of the paper. If a reasonable relationship between the fracture toughness and the tensile properties can be established it will enable the fracture toughness of a material to be determined much more quickly and easily since the estimation of tensile properties is quicker, more straight forward and better established. In addition, the fracture toughness results are employed to evaluate the ability of a theoretical model (Shallhorn 1994) to predict the fracture toughness.

In this thesis, a review of the development of fracture toughness studies of paper, the measurement of fracture toughness using various techniques and the theoretical models proposed to predict fracture toughness is presented in Chapter 2. In Chapter 3, details of the materials, methods, and apparatus are outlined and the experimental set-up of the fracture toughness measurements is described. An image analysis study, carried out to obtain information on the outer plastic deformation zone, is reported in Chapter 4. In Chapter 5, the fracture toughness and tensile properties are compared. Then a new cyclic-loading technique to measure fracture toughness is presented in Chapter 6. Chapter 7 reports a study in which the new technique is used to measure handsheet fracture toughness as a function of the humidity and the level of refining. Finally the major conclusions made in this work and suggestions for further work are presented in Chapter 8.

2 Literature Review

2.1 Introduction

The precise definition of a failure mechanism for paper is not an easy task. Failure can be in the form of a sudden catastrophic event or a slowly decaying breakdown process. A very large collection of literature can be found in the area of strength and failure properties of paper. Frequent paper web failure in manufacturing and converting operations has motivated research in this area. Most of the studies have concentrated on understanding the failure mechanism and in technique development with the aim of improving web runnability.

The study of paper web failure has been often approached from two different ways. One approach is the study of various mechanical properties and comparing these with pilot scale studies of sheet fracture in laboratories, which simulate actual breaks. The other approach is the comparison of sheet mechanical properties with web break statistics, generally in converting operations. However, it is apparent that only a small amount of work has been carried out so far in the comparison of runnability and various fracture toughness measurements. This has mainly been due to the complexity and the time required for these measurements.

In this review of the literature the development and advances in measurement techniques, and in models for the prediction of paper web failure, will be outlined and discussed. In addition basic information will be given on wood fibre structure, inter-fibre bonds as well as important mechanical properties of paper.

2.2 Paper structure

Paper is one of the oldest composite materials, widely used for record keeping, as a medium for communication, printing, packaging and various other applications. Paper is made from a complex network of cellulose fibres bound to each other by hydrogen bonds. The main current source of fibre is from wood but other crops like wheat/rice

straw, sugar cane etc are also used. The fibres from these sources are separated, either mechanically or chemically, during pulping and dispersed in water. The water from this dilute suspension of fibres in water drains through a “wire” (a fabric) leaving fibres behind to form the paper web. The remaining water is then removed by pressing and drying to make the finished paper. The mechanical properties of paper generally depend on the strength of the fibres, the number and strength of the fibre-fibre bonds, as well as the uniformity of the network. Fibres in commercial papers are highly oriented since most of fibres are aligned close to the machine direction (MD) rather than to the cross-machine direction (CD). However, the fibre orientation in laboratory made handsheets is random and the sheets are isotropic.

The wood fibres, the main ingredient of the sheets used in the present study, show visco-elastic characteristics including stress relaxation, creep and strain rate dependence (Baum 1993). Paper also shows visco-elastic properties and can show significant plastic deformation under stress (Seth and Page 1977; Lif and Fellers 1999; Yu, Kettunen et al. 1999).

2.2.1 Wood fibres

The mechanical properties of paper are mainly dominated by the fibre properties. Significant variations in fibre properties occur with wood species and the growth site of the trees. Radiata pine (*pinus radiata*) is the main planted production species in New Zealand and also the principal softwood grown in the plantation forests of Australia. Radiata pine has been considered as one of the more versatile softwoods in the world. In the present work, New Zealand radiata pine bleached market kraft pulp was used in the laboratory sheet preparation.

Although various wood fibres differ in physical and chemical properties, all the fibres have some common characteristics. Figure 2.1 shows the cell wall of a typical “softwood” coniferous tracheid. It consists of different layers and the layer marked as “P” is the primary layer and S1, S2 and S3 are three secondary layers of the wall. The three secondary layers are made of helically wound cellulose fibrils but with different

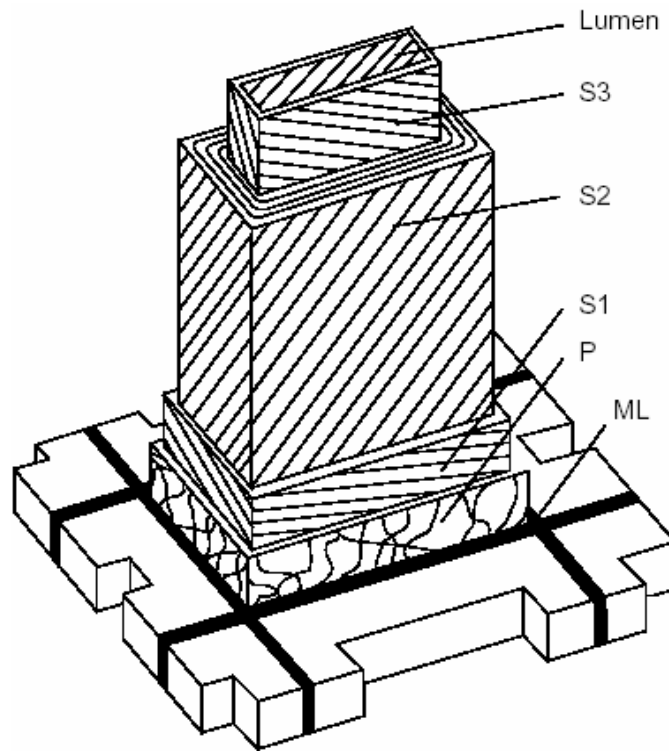


Figure 2.1 Cell wall structure of a typical soft wood (Retulainen, Niskanen *et al.* 1998)

orientation of the fibrils. The outer P and S1 layers are often lost during the pulping process. The S2 layer is the thickest wall component making up the majority of the fibre wall volume and so dominates the mechanical properties of the fibre (Sahlberg, Salmen *et al.* 1997). The S2 layer consists of micro fibrils spirally wound around the fibre axis at an approximately constant fibril angle. The fibrils are primarily tiny bundles of cellulose molecules. In the cell wall fibrils are surrounded by a matrix of amorphous material, which mainly consists of hemicelluloses and lignin. The amorphous matrix is relatively ductile compared to the stiff fibrils and accordingly, it is the fibrils determine the elastic modulus and tensile strength of the fibre in the axial direction. It is believed that the amorphous cellulose is accessible to plasticisers, such as water, which can soften the cellulose components (Salmen and Back 1980). The mechanical properties in the transverse direction of fibre are also important in paper making and refining (Bergander and Salmen 2000).

In a pulping process not only the fibres yield from the wood but also cells generally smaller than fibres can form. These cells form the part of the “fines” fraction of refined pulps (Peel 1999). The addition of fines in a fibre network can increase the bonded and un-bonded area of fibres (Karnis 1995). Fines can consist of cellulose, hemicellulose and lignin. However, the properties of fines can vary significantly from actual fibre fractions (Retulainen and Nieminen 1996; Retulainen, Niskanen *et al.* 1998).

2.2.2 Inter-fibre bonds

Inter fibre bonds play a vital role in the mechanical properties of paper. The nature of inter-fibre bonding is considered complex partly due to the simultaneous operation of several kinds of forces. These forces include chemical bonds within cellulose molecules, intermolecular van der Waals bonds and entanglements of polymer chains. Although it is difficult to make a precise description of bonding, the inter-fibre bonding can be broadly described as the zone where two fibres are so close that chemical bonding, van der Waals interaction occur or molecular entanglement may occur (Retulainen, Niskanen *et al.* 1998). The bonding between paper making wood fibres is considered to be mainly due to hydrogen bonds, which are a special type of chemical bond. Van der Waals bonds also have a small role to play in forming inter fibre bonds. The inter- fibre bonds in a paper gradually form when the solids content of the stock increases during the paper making process. The surface tension forces are important in bringing the fibres close together during the removal of water from the wet web (Robinson 1980). Once the paper is formed in water and dried it is much stronger than when it was wet.

Refining or beating of fibres is performed to improve the mechanical properties of paper. The bonding ability of fibres is improved by refining never dried pulps. It has been long believed that this was the case in the improvement of mechanical properties in previously dried pulps as well. However Page (1989) claimed that the straightening of the fibre during refining is important for the improvement of mechanical properties of paper made from previously dried fibres. This was supported by Seth (2001) who studied the effect of refining on the zero-span tensile strength and showed that the refining process straightens fibres.

Wood fibres tend to shrink during drying, causing a reduction in bonded area. Mechanical properties of a paper sheet will vary depending on whether the sheet dried under external load or without any load. Salmen *et al* (1996) studied the effect of stresses induced due to paper drying on the mechanical properties of inter-fibre bonds using a geometric model. They concluded that when the axial-to-transverse difference in fibre shrinkage is large, then the bonds and hence papers are brittle and can fail at a smaller strain. Inter-fibre bonds can be strengthened by addition of dry strength chemicals and fines (Retulainen and Nieminen 1996).

2.2.2.1 Bond strength

The term “bond strength” is widely used in the paper technology field to describe the structural strength of a fibre-fibre bond system and not just the strength of the interface between fibre-fibre bonds (Uesaka 1983a). Nordman bond strength is another definition given to the specific fibre-fibre bond strength in paper (Page 2002). This was measured by determining the ratio of the non-reversible work during straining a sheet and the change in optical scattering coefficient. However recent work suggested that this ratio does not give a proper measure of the work required to break fibre –fibre bonds as the irreversible work is actually consumed by the fibres as they deform plastically rather than by the inter-fibre bonds (Page 2002; Seth 2002).

Although the concept of bond strength is not well defined it usually refers to the shear strength of the inter-fibre bonds. Shear strength is given as the maximum load that the bond can carry when the bonded fibres are displaced relative to each other parallel to the bonding plane (Retulainen 1998).

2.2.3 Visco-elastic effects

Both fibres and paper have visco-elastic characteristics. A visco-elastic material’s response to an applied stress is partially elastic and partially viscous. A perfectly elastic material stores all of the energy supplied by an external force so that on removal of the force it can return to its original dimensions. In a perfectly viscous fluid, on the other hand, the stress created by external forces relaxes instantaneously to zero because of flow. Polymers are generally considered as viscoelastic materials because they can display the properties of both elastic solids and viscous fluids depending on the temperature or time scale of the experiment (Lakes 2001). Viscoelasticity in amorphous polymers is dependent on the ability of the molecules to flow past each other due the

applied stress (Baum 1993). Figure 2.2 shows the strain response over time of elastic, viscous and visco-elastic materials to a constant applied load.

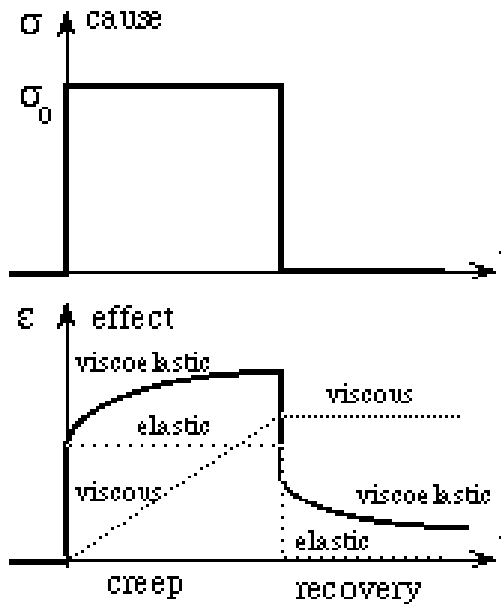


Figure 2.2 Stress (σ) and strain (ϵ) against time (t) for elastic, viscous and visco-elastic materials (Lakes 2001)

The mechanical properties, such as tensile strength, of a visco-elastic material depend on the applied strain rate. A brittle response can be seen at high strain rates compared to a ductile response at low strain rates (Hall 1989).

2.2.4 Effect of moisture

Mechanical properties of paper are also significantly affected by the moisture content. The equilibrium moisture content of paper depends on the ambient relative humidity and the temperature of the surrounding atmosphere. Paper moisture content decreases with decreasing relative humidity (RH) or increasing temperature. The equilibrium moisture content also depends on the moisture and temperature history of the sample. This means that the equilibrium moisture content of paper at a given relative humidity is different in absorption, when coming from dry conditions, and desorption, when coming from wet conditions (Kajanto and Niskanen 1998). The moisture can act as a plasticiser, making changes to the structure and mechanical properties of fibres and paper (Salmen and Back 1980; Steadman and Fellers 1987). In general, plastic deformation will increase and yield strength decrease as the moisture content increases.

2.3 In-plane mechanical properties of paper

Information on in-plane mechanical properties of paper under tension is important in both paper manufacturing and conversion processes since the paper web experiences in-plane stresses in these operations and operating conditions may require adjustment in light of the mechanical properties to obtain the optimum production efficiency. Tensile strength, elastic modulus and TEA are some of the important mechanical properties that are measured for quality control purposes. Apart from these three main mechanical properties, stretch at break, yield stress and the elastic-plastic behaviour of paper are also important.

Tensile strength is perhaps the most common strength test for paper. In a tensile test, a paper sample is loaded in-plane, and pulled apart until failure. The maximum tensile force the specimen can withstand before it breaks and the associated extension of the specimen are recorded. Most of the modern tensile testers record the applied load as a function of extension of the specimen and automatically construct the load-extension or stress-strain curve, an example of which is shown in Figure 2.3. The standard dimensions for a tensile test piece of laboratory made paper is 100 mm long (span) and 15 mm wide.

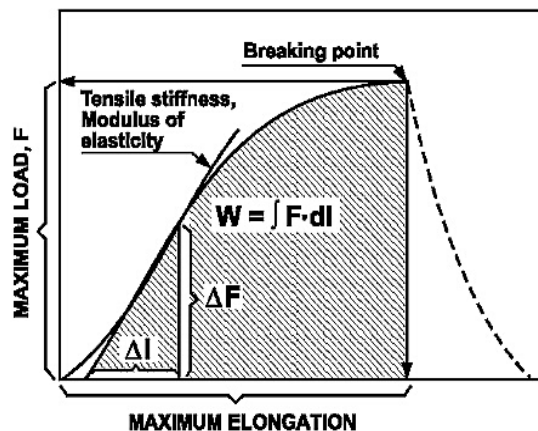


Figure 2.3 A typical load-extension curve for paper showing key points on the curve (Levlin 1999)

2.3.1 Tensile index

The tensile index or specific strength is defined as the maximum load per unit width divided by the basis weight (grammage) of the sheet. The units for the tensile index are Nm/kg.

2.3.2 Elastic modulus

The elastic modulus (E) represents the relative stiffness of the material within the elastic range when the material is under tension. The elastic modulus of paper is a useful property since it controls bending stiffness and the structural rigidity of paper and paper-boards. The elastic modulus can be determined from a stress-strain curve by calculating the ratio of stress to strain ($E = \sigma/\epsilon$) of the linear part of the curve. For non-linear stress-strain curves, the maximum slope $d\sigma/d\epsilon$ is taken as the elastic modulus.

2.3.3 Tensile energy absorption (TEA)

Tensile energy absorption (TEA) determines the work required to break a tensile specimen under tension. This can be determined from the area under a load-extension curve as shown in Figure 2.3. TEA divided by the basis weight gives the TEA index of paper.

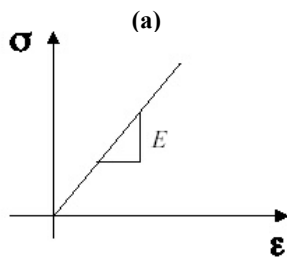
2.3.4 Stretch at break

The stretch at break of a paper specimen gives the maximum extension of a specimen before it breaks. This can be directly obtained from a load-extension curve. Stretch at break divided by the original sample length gives the strain at break of the sample.

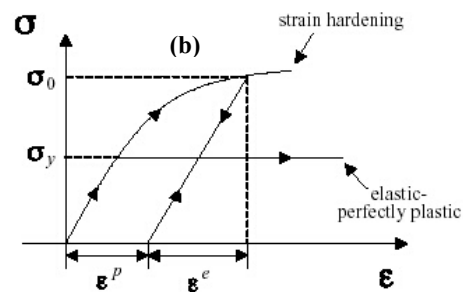
2.3.5 Elastic-plastic behaviour

When a material shows a reversible linear deformation under a load then the material behaves as a linear-elastic or brittle material, as shown in Figure 2.4(a).

• Elastic (brittle) material:



• Plastic (ductile) material:



ϵ^e : elastic strain σ_y : "initial" yield stress
 ϵ^p : plastic strain σ_0 : current yield stress

Figure 2.4 Load-extension behaviour of linear-elastic (a) and elastic-plastic material (b) (Lambros 2002)

All the energy applied to strain the material is recovered upon release of the load. However, a material like paper yields at a certain load and deforms irreversibly upon further straining. Its load-extension curve deviates from linearity as shown in the Figure 2.4(b).

2.3.6 Yield stress

The stress-strain proportional limit (or linear limit) of the stress-strain curve gives the yield stress of a material. It is expected that a specimen will behave as a linear-elastic material until it reach the yield stress. The material then plastically deforms when the applied stress is above the yield stress. However, for paper the yield stress is not well defined, because there is no clear transition from the linear region to the non-linear region. Although yield stress in paper is not a well defined quantity, it is commonly taken at the point where strain deviates by 0.2% from a linear trend fitted to the start of the load-displacement curve (Niskanen & Karenlampi, 1998). For the purpose of this thesis, a ligament of a sample is described as fully or completely yielded when this level of plastic strain is exceeded across the whole ligament.

2.4 Paper runnability

Generally all materials contain localized weak spots and paper is no exception. These weak spots or defects in paper can originate from shives, calender scabs, hairs, holes, stickies, plastics etc. In the literature, a significant consideration has been given to shives, since there had been some correlation found between web breaks and the number of shives in newsprint. A shive is a bundle of fibres that is poorly bonded with the rest of the sheet (see Figure 2.5a) and these defects or flaws in the sheet can act as cracks.

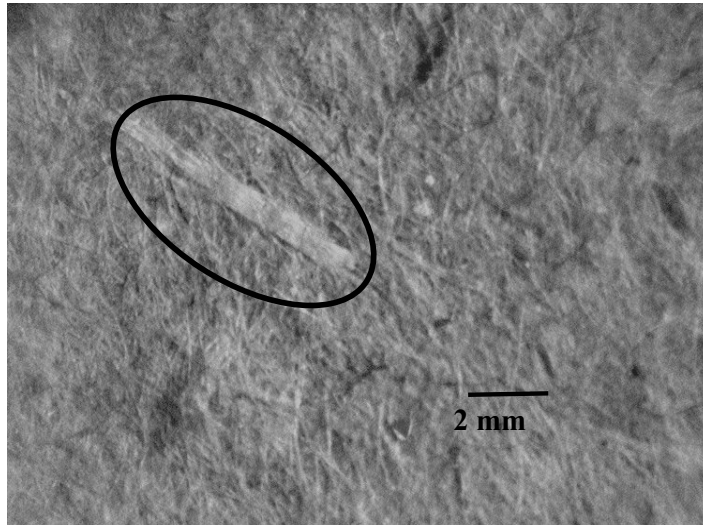


Figure 2.5a Optical microscopic image of a shive incorporated in a unbleached kraft hand sheet

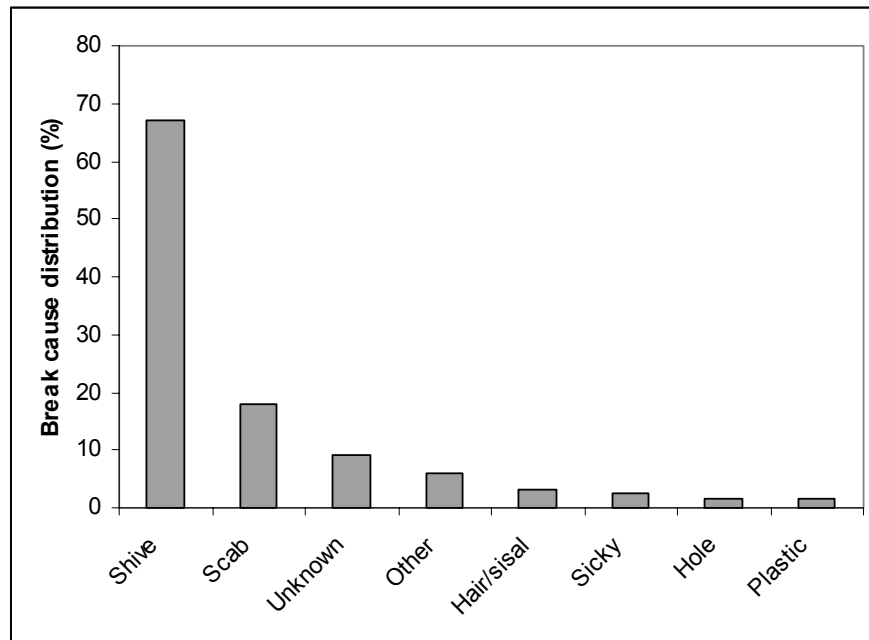


Figure 2.5b The distribution of defect contribution to web failures in newsprint (Adams and Westlund 1982)

Under load these small cracks can extend and produce catastrophic web failure. Figure 2.5b shows a distribution of breaks initiated from various sources in newsprint obtained from pilot scale studies (Adams and Westlund 1982). It is an obvious fact that the paper web breaks can severely impair paper machine and converting efficiencies. Web breaks can be costly to the industry in terms of finance, production efficiency and product

quality. The requirement to improve the web efficiency by minimising breaks has always been considered as one of the key tasks in paper industry research.

The efficiency of paper web manufacture or conversion is commonly described by paper web “runnability” in manufacturing or converting operations. The usual definition of this term is the “expected mean frequency of web breaks for a given material per 100 rolls” (breaks/100 rolls). However, in some cases, runnability has been estimated as the number of breaks per sheet length or per sheet area. Many studies indicated that defects such as shives in the paper impact the runnability of the paper web (Moilanen and Linqdvist 1996; Swinehart and Broek 1996; Gregersen, Hansen et al. 2000; Fellers, Malander et al. 2001; Koskinen, Kosonen et al. 2001). In opposition to these studies, Uesaka *et al* (2001) reported that available data from printing and other converting operations were insufficient to claim any significant effect of shives on web runnability. In a previous work they reported that unless the macroscopic defects in a sheet such as holes, cuts, shives etc. were quite large, then under normal operating conditions web breaks will rarely occur due to such defects (Uesaka and Ferahi 1999).

Paper runnability is also strongly dependent on the moisture content of the paper (Roisum 1993). It is known that when the moisture content of the paper is low then the paper is brittle and fails easily. Further, cyclic humidity variation could improve stress relaxation allowing the paper to be stretched more, thus improving runnability (Kimura, Usuda *et al.* 1977). The load applied to the paper web in the operation is another important parameter affecting runnability. In manufacturing, printing and other converting operations most of these loads are applied in the plane of the sheet.

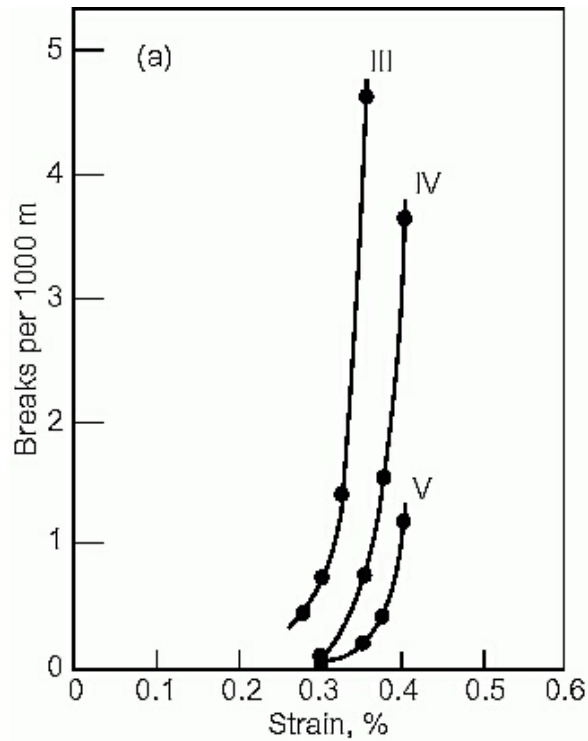


Figure 2.6 Number of web breaks per 1000 m as a function of web tension. The labels, III, IV and V represent different commercial papers (Sears, Russell *et al.* 1965)

It has been reported that web break frequency is related to the operational web tension (Sears, Russell *et al.* 1965; Eriksson 1987; Roisum 1990), the tension variability across the web (Linna, Parola *et al.* 2002) and also along the length of the web (Roisum 1990). The average web tension is generally much lower than the average tensile strength of the paper. The combination of variations in the local strength of the paper and temporary fluctuations in the local loads is then the main cause for such breaks. Figure 2.6 shows the exponential dependence of newsprint web break frequency on the strain measured with a winding instrument running at 366 meters per minutes (Sears, Russell *et al.* 1965). The labels, III, IV and V shown next to the curves in figure represent the different commercial papers that were used in these experiments.

It is certain that there is a relationship between tension and web breaks, but the exponential relationship reported by Sears, Russell *et al.*, (1965) has not been well established and hence cannot be used to predict converting efficiency. It is clear that tensile loads play a significant role in paper runnability, and some correlation between tensile strength and runnability was obtained (Uesaka, Ferahi *et al.* 2001). There have

been a number of methods used in the characterization of paper runnability. Section 2.6 gives a brief review of the runnability studies.

2.5 Historical development in paper web runnability studies

A significant improvement in runnability has been achieved during the last three decades by adopting effective screening of pulp, on-line monitoring of web defects and careful control of web tension and operating conditions (VTT-IT 2001; MetsoAutomation 2002). These improvements in runnability have been used to increase production by increasing web speeds. However, even with all these precautions and improvements, paper web failures are still common in the industry. Paper web runnability studies are carried out essentially to determine the factors affecting runnability, machine performance and paper quality. Since web breaks are very infrequent events, a lack of quantitative data makes the runnability studies extremely difficult. However, one method of evaluating runnability is the statistical data collection from paper mills, pressrooms and other converting operations and analysing this data to find the cause of the web breaks. Mathematical modelling and pilot-scale lab runnability tests to simulate actual situations are the other methods used to evaluate runnability.

2.5.1 Statistical data collection

Although statistical correlation of break frequency with any paper property is difficult and time consuming, some attempts have been made. Linna *et al.* (2002) studied the correlation between web breaks and the web tension profile in the cross-machine direction of the paper web. They reported that the paper machine web tension profile was convex in shape and high break rates occurred at low as well as at high tensions. They claimed that the web breaks at high tensions were due to the limited paper strength caused by defects in the paper. The effect of low tension on the break rate was explained as due to wrinkling and instability of the web. Uesaka *et al.* (Uesaka, Ferahi *et al.* 2001) collected data in three pressrooms for a number of years and attempted to correlate break rate and strength properties. They noted the need for precise statistics to make clear conclusions.

After analysing data collected over several decades, (Page and Seth 1982) reported that a large amount of break data (1000 to 10000 rolls) is required even to distinguish

between papers obtained from different manufacturers. They further showed that breaks occur at random intervals and are due to a number of random disturbing factors. As such, the number of breaks per given number of rolls obeys a Poisson distribution. Analysis of such a huge set of data could take months and by this time the paper properties could significantly change from humidity, temperature and other factors. In addition, humidity fluctuations in pressrooms produced more significant runnability variations than the differences observed in paper from different manufacturers (Page and Seth 1982; Roisum 1989). These reasons restrict the usefulness of runnability estimation using statistical data collection. Therefore a reliable and efficient technique is necessary to determine the web runnability.

2.5.2 Mathematical modelling

Studies of statistical data show the difficulties with the method to obtain definite conclusions. Therefore mathematical models have been developed and tested to simulate manufacturing and pressroom web breaks and hence to predict the runnability. Uesaka, Ferahi (1999) and Uesaka, Ferahi *et al*, (2001) developed a probability model to identify principal factors controlling web breaks in press rooms. The results obtained from the model suggested that most of the pressroom web breaks occur because of tension variations rather than the small defects or weak spots in paper. Gregersen (1998) and Gregersen & co-workers (1998) evaluated the newsprint strength and runnability by using Weibull statistics. Weibull statistics are often used to design products fabricated from brittle materials and to estimate the cumulative probability of the failure of a given sample under a given load and is based on the main assumption that local strength variation is randomly distributed. However, Gregersen *et al* found that evaluation of newsprint strength by Weibull statistics didn't provide satisfactory results due to the fact that the local strength variations of are not randomly distributed.

Although it is possible to develop a reasonable semi-empirical model to predict the frequency of web breaks by including the main parameters that affect the paper strength, it is less likely that a such a model will replace the direct use of a failure characterisation technique as the large number of parameters may mean that the prediction of failure in a production and converting environment may not be very practical.

2.5.3 Pilot tests

In addition to statistical data collection and mathematical modelling, pilot-scale lab runnability tests have been performed to simulate mill and print room operations and to forecast paper web failures (Sears, Russell et al. 1965; Adams and Westlund 1982; Roisum 1990; Uesaka, Ferahi et al. 2001). In these methods, large samples of web run at low tensions and small samples run at high operating tensions were investigated. Much valuable information has been gained from these studies. However, these tests are also time-consuming and require heavy equipment to perform the measurements.

2.6 Correlation of basic mechanical properties with runnability

It was understood that interpreting break records are difficult in the short term because there were large random variations in the collected data. On the other hand, long-term data is affected by other factors, such as humidity, which complicate the analysis. Mathematical modelling and pilot tests also didn't give accurate runnability predictions. Thus attempts were made to find relations between strength properties and the paper runnability. Preliminary experiments carried out by Page and Seth (Page and Seth 1982) found that there were no statistical differences in the strength tests carried out on paper from rolls which had breaks and rolls which had no breaks. This supported the concept that defects are a major cause of breaks. Furthermore, it was found that the fracture resistance was constant for any series of rolls from one mill but varied significantly from mill to mill. They concluded that strength depends mainly on the manufacturing conditions and the furnish composition.

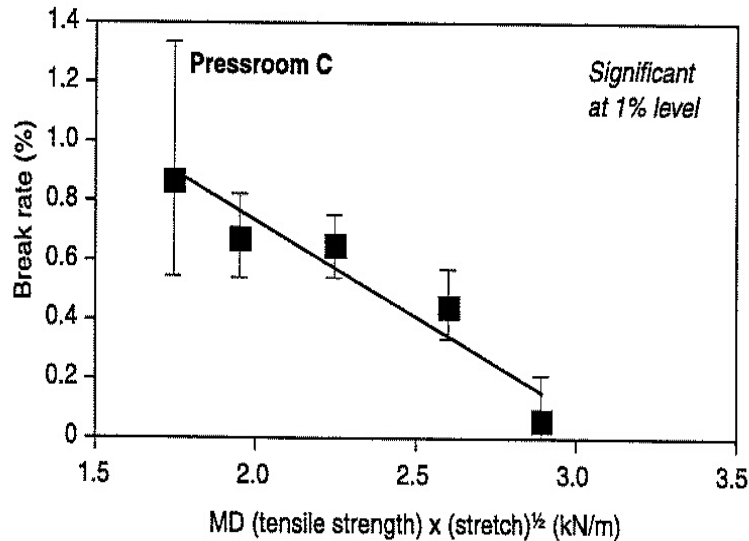


Figure 2.7 Break frequency versus combination of tensile parameters (Uesaka, Ferahi *et al.* 2001)

A more significant relation between runnability and strength properties was recently reported (Uesaka, Ferahi *et al.* 2001). They examined three criteria to test the relationships between strength properties and break rates. They used the criteria to confirm whether the relationship was statistically significant and also to see whether there was a single variable that controlled the web breaks. The criteria were (1) whether the break frequency varies with the strength property, (2) if it varies whether the variation is linear, (3) if it is linear, whether the slope is statistically significant. Figure 2.7 shows the correlation between break rate and a combination of tensile strength and stretch. Uesaka *et al.* reported that tensile strength had the most statistically significant, linear relationship with break rate when compared to other properties like TEA, stretch, tear and burst index. The combined parameter of strength x stretch^{1/2} also showed a good linear correlation with break rate. However, they couldn't test the correlation of fracture toughness to web breaks, as fracture toughness had not been measured.

2.7 Tear strength as a web break controlling parameter

It has been understood that the paper runnability or flaw carrying ability of paper should be characterised as a material property. The flaw carrying ability has been defined as the resistance offered by the sheet to the propagation of a crack initiated by a flaw (eg., a shive) in its structure. The tearing of paper consumes energy and the energy consumed to propagate a tear has been assumed to correlate with the flaw carrying

ability of the paper. In this context, if a large amount of energy is consumed for the propagation of a pre-existing crack in one material compared to another material, the former material is assumed to be less likely to fail under a given load.

As a conventional practice the tear strength of paper has been used in the industry as a measure of runnability. Both out-of-plane Elmendorf or Brecht-Imset tear tests (Chatterjee, Kortschot *et al.* 1993; Seth 1996) and in-plane tear tests (Seth and Page 1975; Karenlampi, Suurhamari *et al.* 1996; Retulainen 1996; Yu, Kettunen *et al.* 1999) are carried out to characterise the materials ability to resist sheet fracture.

2.7.1 Elmendorf tear strength

In many countries, the Elmendorf tear test is routinely employed as a measure of runnability. The Elmendorf test method essentially involves applying an impact load to pull the sample apart normal to the plane of the sheet (see Figure 2.8). The tear index measures the work consumed in either breaking the fibres or pulling them out from the fibre network. It had been supposed that the energy consumed in extending a crack in paper would correlate with runnability.

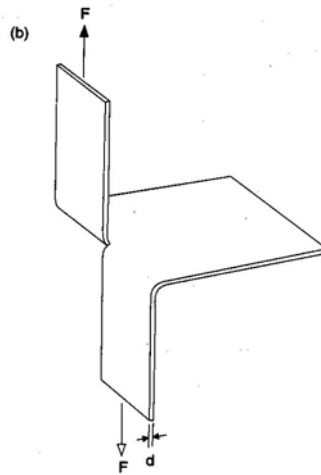


Figure 2.8 Out-of plane tear test (Niskanen and Karenlampi 1998)

Although different standard test methods recommend slightly different procedures for a out-of plane tear test, the fundamental principle involved is the same, whereby a paper sample is clamped between two split jaws, and a cut is made using a sharp blade. This produces a crack in the sample at which tear is initiated.

Although the Elmendorf tear index has been considered an important mechanical parameter to quantify the runnability, there have been doubts over its usefulness (Seth *et al.*, 1993). The main reason for this is that its mode of failure is not comparable to that of most of the actual web failures. In general, three basic modes of failure have been described in fracture mechanics, as shown in Figure 2.9. Mode I is a tensile (or cleavage) failure and this is the most relevant mode of failure for most paper web breaks. Mode II is an in-plane shear or sliding mode of failure. This kind of a failure can occur inside a wound roll of paper as a shear burst (Lyne, Jackson *et al.* 1972). The Elmendorf tear test falls under failure mode III, which describes an out-of-plane, shear type failure. Although the out-of plane tear test measures the sheet resistance in the shearing or torsion-tearing mode of failure, it does not simulate the fracture of a moving

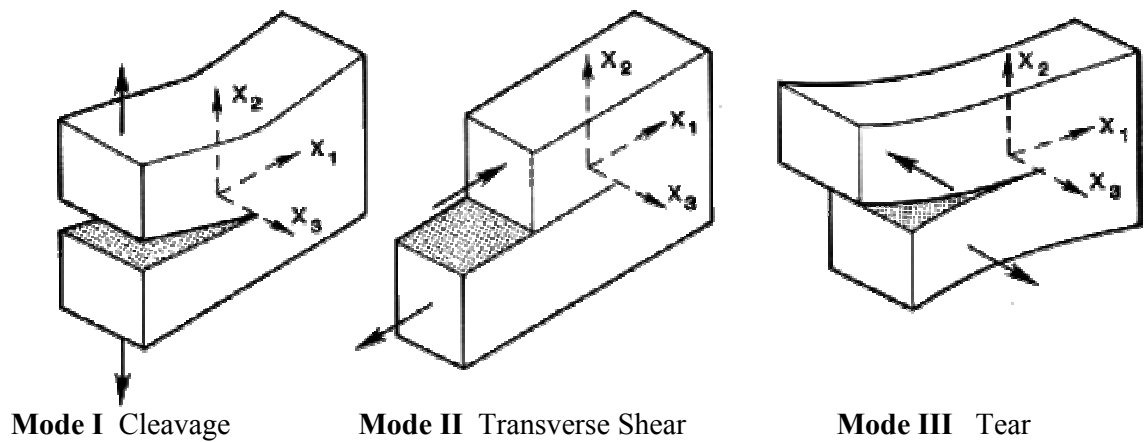


Figure 2.9 Failure modes of a material

web in manufacturing or converting (Seth 1996). As the mode of failure in an Elmendorf tear test is different to that of a moving web, an in-plane tear test was developed, which was expected to provide more relevant information.

2.7.2 *In-plane tear test*

Van den Akker *et al.* (1967) developed a technique to measure the in-plane tear of paper. This technique involves inserting a small edge notched sheet in a pair of clamps in a misaligned configuration such that each clamp is rotated through 6° in the plane of the sheet, as shown in Figure 2.10.

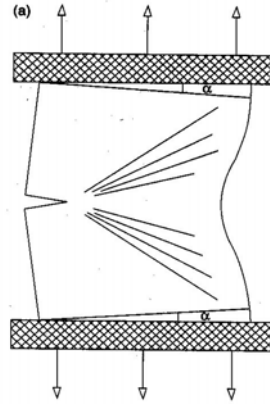


Figure 2.10 In-plane tear sample configuration (Niskanen and Karenlampi 1998)

The clamps are then pulled apart to initiate the tear from the notch and complete it in the plane of the sheet. Although an in-plane tear test can be considered as a Mode I failure, it is not a pure in-plane test because of wrinkling of the sheet caused by the sample's buckled state.

Lyne *et al.*, (1973) studied the relationship between the Elmendorf and in-plane tear tests as a function of sheet density for two different types of sheets. After an initial peak, a large reduction with beating was seen in the Elmendorf tear, while in-plane tear either increased or stayed approximately the same. Karenlampi (1996b) and Karenlampi *et al.*, (1996) studied the relationship between fibre length and in-plane tear index and concluded that in-plane tear index was linearly proportional to fibre length and bond strength. Kettunen *et al.* (2000) measured the in-plane tear energy as a function tear angle. They claimed that the decrease in tear work, with increasing tear angle, is due to a decrease in the work consumed in the outer plastic zone. However, the actual tearing mechanism could be complex than it appears, due to type of paper grade and tear angle (Kettunen and Niskanen 2000).

Although both the Elmendorf and in-plane tear strength of paper, have been employed as a measure of runnability, there has been no well established relationship between runnability and either tear strength (Larocque 1962; Page and Seth 1982; Roisum 1990; Niskanen 1993). At the same time the relevancy of the in-plane tear technique has been questioned, since it involves a 12° tearing angle and this is not similar to actual web failure (Seth and Page 1975; Kettunen and Niskanen 2000).

Neither the out-of plane nor in-plane tear tests measures the required property since the sample is not strained in mode I, which ultimately governs the failure. In order to characterize paper runnability, a reliable technique is required to measure the paper's ability to resist fracture in the presence of small defects, while being loaded in mode I.

2.8 Application of fracture mechanics to predict sheet failure

Any technique used to characterise the flaw carrying ability of a paper web should measure an intrinsic property of the material. In general, flaw-carrying ability can be defined as the resistance offered by the paper sheet against stable or unstable crack growth initiated from a defect or flaw in its structure. Stresses can concentrate at a boundary of a flaw and this can lead to local rupture. When the stress reaches some critical value the crack can enlarge and under certain conditions it will propagate through the material.

Given that the Elmendorf tear or standard in-plane tear tests cannot measure such a property of paper, attention had been focused on other available techniques that can predict the paper failure properties in a pure tensile mode. As linear elastic fracture mechanics has come into widespread use as an engineering science tool, attempts were made to use this technique to characterise paper web failures.

2.8.1 Linear Elastic Fracture Mechanics (LEFM)

The linear elastic fracture approach assumes that a material is behaving as a pure linear-elastic object. This means that the material can be strained reversibly as shown in Figure 2.4(a). The LEFM analysis has used two main approaches. One is based on Griffith fracture theory and the other approach is based on the mathematical analysis of the stress concentrations at a crack tip, hence defining the concept of stress intensity factor. The following paragraphs briefly outline these techniques and their application to the fracture of paper.

2.8.1.1 Griffith's theory of fracture

A. A. Griffith has made a significant contribution to the present development of our understanding of fracture and failure properties of materials. Although fracture mechanics has mainly progressed since the middle fifties, Griffith's theory on fracture has been considered as a starting point in this field. Since the application of this

fracture theory was successful to brittle materials, Andersson and Falk (1966) first investigated the applicability of this theory to paper.

Griffith fracture theory is based on a thermodynamic energy balance approach. When a load is applied to a specimen with a crack, the externally added energy due to the applied load and the resulting elongation must be equal to the sum of the increase in internally stored energy and any increase in surface energy occurring if the crack has been extended. The theory assumes that the material is entirely elastic and that the creation of fracture surface consumes a certain amount of energy per unit crack area, which is twice the surface energy of the material, γ . When an elastic specimen with a crack is stressed, a balance must be reached between the decrease in potential energy U (related to the release of stored elastic energy), and the increase in surface energy S . For a sample with a elliptical crack of length $2a$, and thickness t , situated in an infinite body and lying normal to the applied tensile stress (the configuration shown in Figure 2.11), Griffith showed that the decrease in potential energy of this cracked specimen is $(\pi\sigma^2 a^2 t)/E$. Here σ is the applied stress, t is sample thickness and E is Young's modulus.

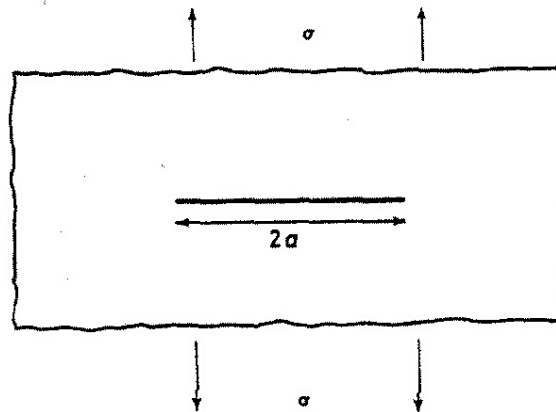


Figure 2.11 An infinite body with a crack of length $2a$. The loads are applied in a tensile mode (Knott 1973)

By considering a half length of the sample), the total energy (W) of the sample can be written as (in plane stress);

$$W = U + S = -1/2 (\pi\sigma^2 a^2 t)/E + 2\gamma t a \quad \mathbf{2.1}$$

Considering the equilibrium condition, the minimum in total energy can be obtained by setting $\partial W/\partial a = 0$, which gives the relationship,

$$2\gamma = \frac{\pi\sigma^2 a}{E} \quad 2.2$$

For a given crack length (a), the Griffith fracture stress is then given by

$$\sigma_F = \sqrt{\left[\frac{2E\gamma}{\pi a} \right]} \quad 2.3$$

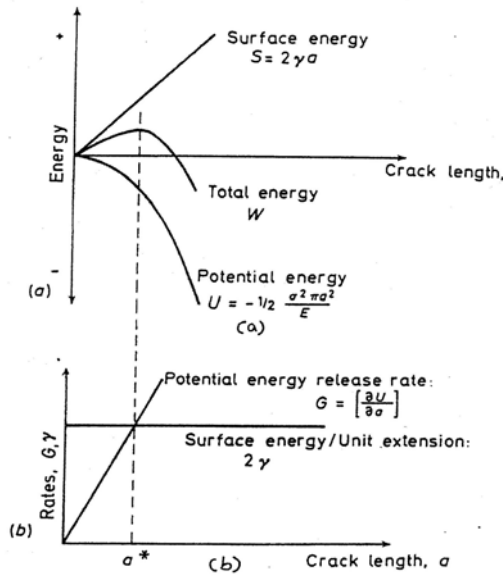


Figure 2.12 (a) Surface energy and potential energy contribution to the total energy according to the Griffith fracture criterion **(b)** Energy release rates versus crack length (Knott 1973)

Figure 2.12a shows the surface energy and the potential energy contribution to the total energy. The intersection of the line $-(\partial U/\partial a) = \sigma^2 \pi a/E$ with $(\partial S/\partial a) = 2\gamma$ shown in Figure 2.12b is a visualisation of equation (2.2). In general, the positive value of the gradient $(\partial U/\partial a)$ is defined as the strain energy release rate (G) with respect to crack length (Knott, 1981).

$$G = -(\partial U/\partial a) \quad 2.4$$

The crack can propagate, if the available energy equals or exceeds the critical (characteristic) energy, G_c , of the material.

$$G \geq G_c$$

2.5

The two quantities G and G_c are quite distinct in their characteristics. The strain energy release rate (G) depends on sample geometry, loading conditions and its elastic properties while G_c is the energy absorbed by the body in the crack extension process. This is a material property and hence can be used to evaluate the fracture resistance of the material.

2.8.1.2 Stress intensity approach

The stress intensity approach characterizes the stress concentration at the tip of crack in terms of a factor K , the stress intensity factor. The applied load, crack geometry and the specimen geometry are taken into consideration when describing the state of the stress at the vicinity of the crack-tip by using the factor K .

In a similar manner to the strain energy release rate, a critical stress intensity factor can be defined at the point where the sample begins to fracture. This critical stress intensity factor, K_c , is sometimes called the “tenacity” (Swinehart and Broek 1995). For an elastic sample containing a centre crack, under a critical tensile stress (σ_c) in the plane stress opening mode (mode I) K_c is given (Paris and Sih 1965) by;

$$\sigma_c = K_c / \sqrt{(\pi a)} F(a/b) \quad \mathbf{2.6a}$$

or

$$\sigma_c = K_c / \sqrt{\beta a} \quad \mathbf{2.6b}$$

where $2b$ is the sample width and $2a$ is the crack length at instability. $F(a/b)$ is a finite-width correction factor and is unity for an infinite plate. β is a geometric factor that depends on the crack size a and the web width. Application of linear elastic stress analysis techniques is generally valid for brittle materials and the stress intensity factor, K_c , is independent of crack length for such materials. However it was found that most of the materials studied showed some plastic deformation around the crack tip just before the fracture. Irwin (Irwin 1957) therefore proposed a correction for small scale yielding around the crack tip, where in such an instance, the elastic stress intensity approach still could be justified.

2.8.1.3 Irwin's model for crack-tip plastic-zone estimation

Whenever the applied stress exceeds the yield strength (σ_{ys}) of the material, plastic deformation around the crack tip prior to fracture is expected. The stress (σ_T) at a distance, r , and angle, θ , from the crack tip (see Figure 2.13) is given by,

$$\sigma_T = \frac{K}{\sqrt{2\pi r}} \cos \frac{\theta}{2} \left(1 + \sin \frac{\theta}{2} \sin \frac{3\theta}{2} \right) \quad 2.7$$

If the crack propagates in the direction $\theta=0^\circ$, then the stress will be $\sigma_T = \frac{K}{\sqrt{2\pi r}}$. The stress will exceed the yield strength at some distance r_y from the crack-tip as shown in Figure 2.13. At the elastic-plastic boundary, $\sigma_T = \sigma_{ys}$ (yield strength), and hence the plastic zone is given by,

$$r_y = \frac{1}{2\pi} \left[\frac{K}{\sigma_{ys}} \right]^2 \quad 2.8$$

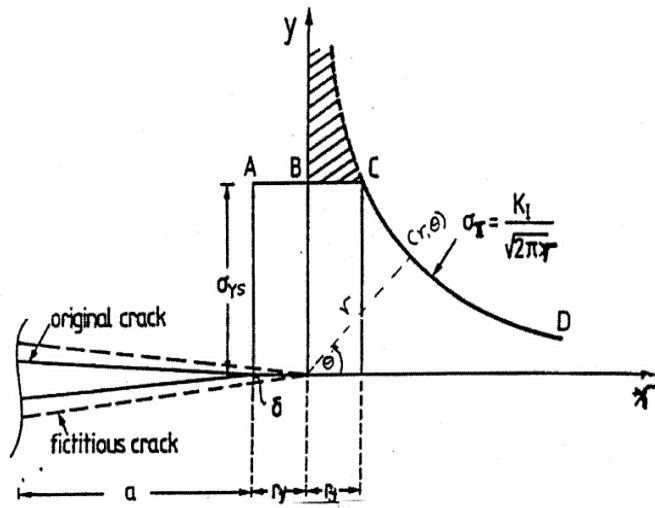


Figure 2.13 The stress distribution and crack-tip correction according to Irwin's model (Gdoutos 1993)

The presence of a plastic region makes the material behave as if it has a crack length that is slightly longer than the actual length. The effective crack length is assumed to be the actual crack length plus some fraction of the plastic-zone diameter. As a first approximation, Irwin set this increment equal to the radius of the plastic zone, so that effective crack length would be $(a + r_y)$. Therefore the effective critical stress intensity factor is given by,

$$K_c(\text{effective}) = \frac{\sigma_c \sqrt{\pi a}}{\left[1 - \frac{1}{2} \left(\frac{\sigma_c}{\sigma_{ys}}\right)^2\right]^{1/2}} \quad 2.9$$

As a way of simplifying estimation of the critical strain energy release rate G_c , Irwin proposed that for an isotropic material in plane stress, K_c and G_c are related by

$$G_c = K_c^2/E \quad 2.10$$

where E is the elastic modulus of the sample. Although in the case of a homogeneous orthotropic material, the stress intensity factor K_c in the plane stress opening mode remains the same, the expression for the critical strain energy release rate (for a crack propagating parallel to a plane of elastic symmetry) has to be modified to (Sih, Paris *et al.* 1965)

$$G_c = K_c^2 \left[\frac{a_{11}a_{22}}{2} \right]^{1/2} \left[\left(\frac{a_{11}}{a_{22}} \right)^{1/2} + \frac{2a_{12} + a_{66}}{2a_{22}} \right]^{1/2} \quad 2.11$$

In this equation, the a_{ij} are the elements of compliance moduli of the sample. The estimation of G_c involves measuring the critical failure stress, yield stress and elastic constants for a sample with known crack length. However, it is experimentally tedious to obtain all these parameters and constants to evaluate the critical energy release rate (which is called the crack extension force by some workers) for a particular sample. Therefore, Gurney and Hunt (Gurney and Hunt 1967) proposed a “quasi-static-crack propagation approach” which simplifies the estimation of G_c .

2.8.1.4 *Quasi-static-approach*

The main condition required for this approach is that the crack growth should be stable. According to the Griffith fracture criterion, when an elastic sample fulfils equation 2.5, such that the energy being released is equal to or greater than the sample’s characteristic energy, then the crack can grow. However, whether the subsequent crack growth is stable or unstable depends on whether the energy supply, $(-\partial U / \partial a)$, increases or decreases with the increase in crack area. If the increase in supply energy with the

increase in crack area is greater than the energy required to create new surfaces (i.e., $-\partial^2 U / \partial a > \partial^2 W / \partial a^2$), the crack growth is unstable. However, if during crack propagation, the increase in supplied energy is less than the increase in required energy, the crack will stop or stabilise. It is therefore necessary to supply additional energy to obtain further crack growth. This condition has been identified as a quasi-static situation and allows for G_c to be directly experimentally evaluated.

The quasi-static condition has been applied to paper (Seth and Page 1974; Seth and Page 1975; Pouyet, Volozinskis et al. 1989; Tryding and Gustafsson 2001) and the energy transmitted to the sample to produce a unit increase in the crack area has been obtained. Details of these tests are discussed in section 2.8.2.2.

2.8.2 Application of LEFM to paper

Application of the LEFM to paper to measure fracture toughness is not simple, because the elastic energy release rate, G , can easily go over the critical value G_c . However, considerable progress has been made in the application of LEFM in paper (Seth and Page 1974; Seth 1979; Swinehart and Broek 1995; Ferahi, Kortschot *et al.* 1996; Swinehart and Broek 1996). LEFM has, in general, only been successfully applied to quite brittle papers such as bond paper or newsprint.

2.8.2.1 Measurement of K_c

Although there is no standard procedure for the estimation of K_c , two conditions seem to be critical in order to successfully make the measurements. The first condition is that the yield stress (σ_{ys}) of the sample should be greater than the net effective stress applied to the specimen (σ_N) over the un-cracked region at failure (ASTM, 1964). The second condition is that the sample dimensions should be large enough to avoid any sample boundary interferences with the crack-tip stress distribution (McClintock and Irwin 1965). These conditions have mainly been met by choosing a sufficiently large specimen and selecting a suitable crack length, but the correct dimensions can be determined only by experiment. Srawley and Brown (Srawley and Brown 1965) suggested measuring K_c over a range of specimen widths in order to obtain the true K_c without any boundary interference.

Seth and Page (Seth and Page 1974) conducted tests and obtained K_c for various types of paper. Samples with symmetric double cracks were prepared and widths were varied

over the range $2b = 5$ to 50 cm. The sample length to width ratio (l/b) and crack length to sample width ratio (a/b) were set to 3 and 0.35, respectively for $5\text{cm} < 2b < 10\text{cm}$. For samples with dimensions: $15\text{cm} < 2b < 50\text{cm}$, l/b was set to be 1.0 and a/b was set to 0.4. The initial crack-length and peak load obtained from a load–extension curve were used to estimate K_c . Separate tests on 3.8cm wide tensile test samples were carried out to estimate yield stress. The yield stress was defined as the stress where the strain deviated by 0.2 % from linearity.

Figure 2.14 and Figure 2.15 show the results obtained by Seth and Page for σ_N/σ_{ys} and K_c as functions of the specimen width, b . The σ_N/σ_{ys} ratio was below unity for samples prepared with $2b$ above 10 cm, thus satisfying the first condition. In Figure 2.15, the results obtained for bond paper 1 and bond paper 2 clearly showed the influence of sample width on K_c . A relatively constant value of K_c was obtained only for samples having $2b > 18\text{cm}$. This indicates the importance of choosing a relatively large specimen width to obtain a constant K_c , which does not depend on sample geometry. The critical strain energy release rate (G_c) of these samples was calculated using Equation 2.11.

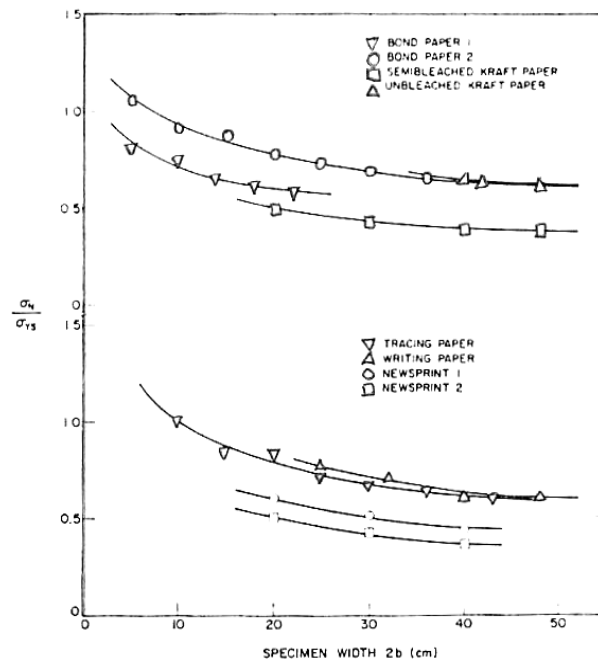


Figure 2.14 σ_N/σ_{YS} against sample width ($2b$) of different papers (Seth and Page 1974)

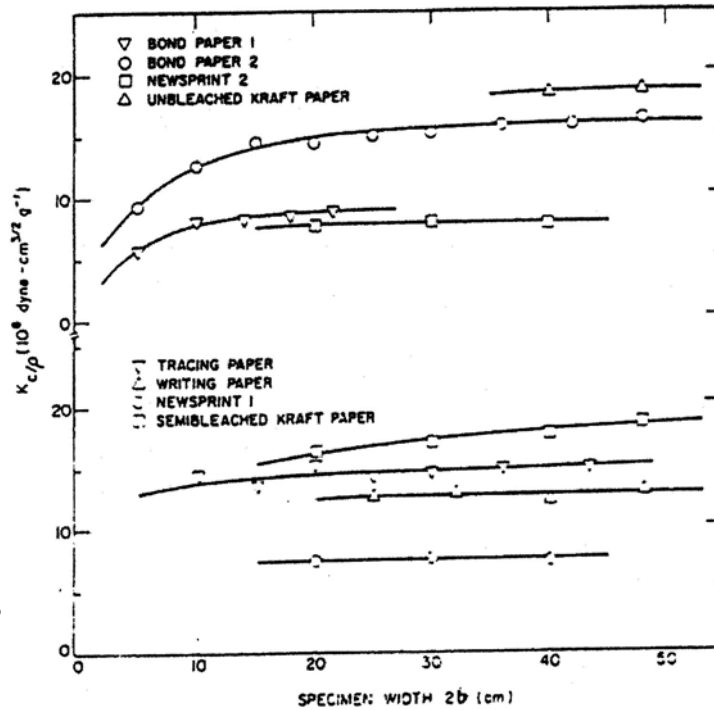


Figure 2.15 K_{cI}/ρ against sample width for the samples shown in Figure 14 (Seth and Page 1974)

Swinehart and Broek (1995) investigated the advantages and disadvantages of determining fracture toughness of paper using either stress intensity factor (K) or strain energy release rate. They claimed that K is more useful since the geometric factors for complicated geometries in paper can be easily obtained. Their results showed that the relationship between failure stress (σ_c) and crack size ($2a$) was in good agreement with equation (2.6b) if the crack size is large as shown in Figure 2.16. Although there was a good agreement between the predicted and the experimental values, the applicability of equation 2.6b was questioned because the defects in paper webs are smaller than the crack lengths that showed good agreement with the equation (Niskanen and Karenlampi 1998).

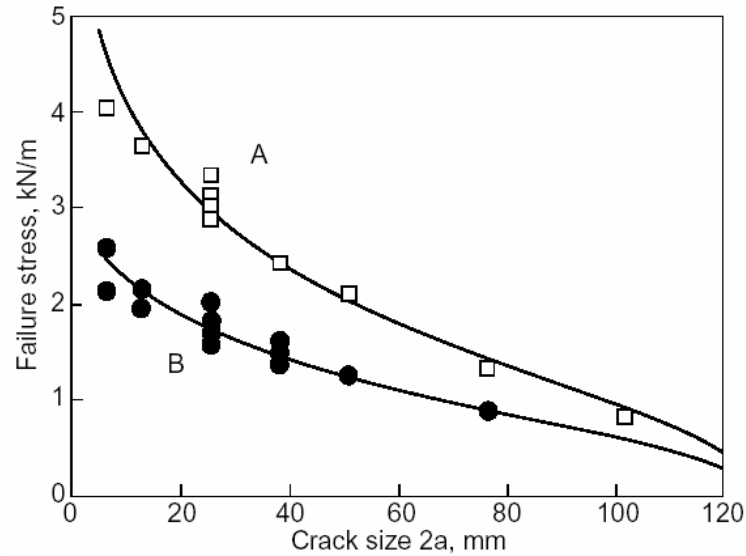


Figure 2.16 Critical failure stress against initial crack length for two different bond papers. The solid lines are corresponding predictions from equation 2.6 (Swinehart and Broek 1995)

Ferahi *et al* (Ferahi, Kortschot *et al.* 1996) applied LEFM in newsprint to investigate shive-initiated breaks. This approach was not successful and they claimed that in highly oriented material like paper, the directional variation of fracture toughness should be considered to obtain reliable results.

2.8.2.2 Work of fracture (R)

Following a quasi-static approach, Seth and Page (Seth and Page 1974) tested the same paper samples shown in Figure 2.15 to obtain the work of fracture (R) as a means of estimating the fracture resistance. One of the basic conditions that needed to be satisfied for the application of this approach was that the energy stored in the specimen and the testing machine at the time of failure is small, so as to avoid any catastrophic failure.

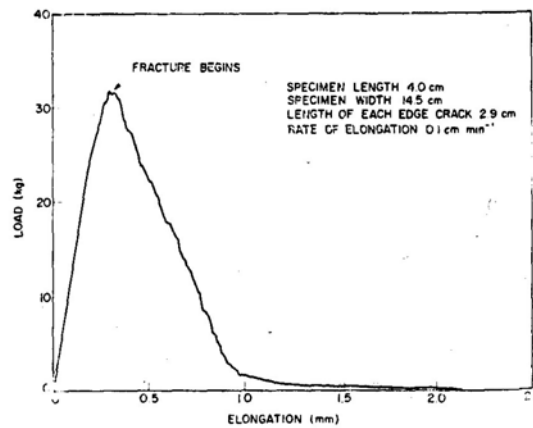
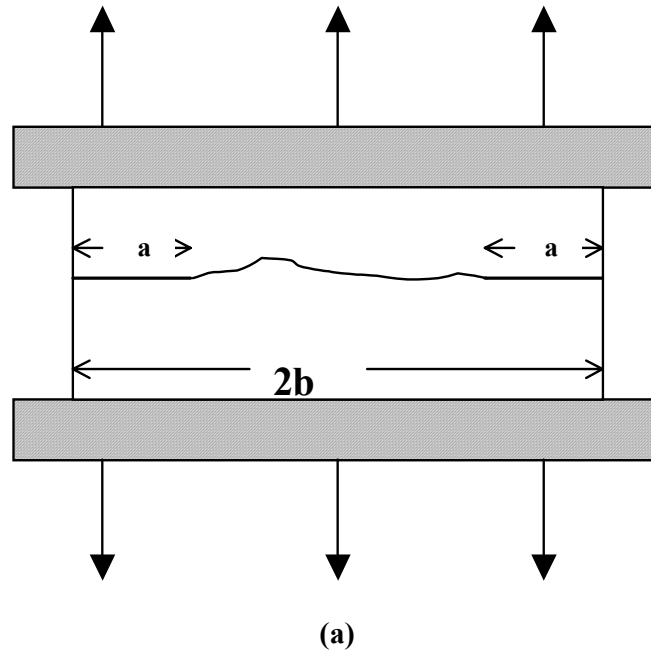


Figure 2.17 (a) Short wide tensile specimen (as wide as 20 cm) used in quasi-static approach **(b)** The typical load-extension curve for a quasi-static crack propagation

The other important condition is that suitable crack and specimen dimensions must be selected such that at failure, the net stress away from the crack-tip does not exceed the sample yield strength. The use of a Instron model universal testing machine and short but wide tensile specimens (up to 20cm, - see Figure 2.17a) with symmetric edge notches clamped into two line type clamps enabled these conditions to be satisfied. Selection of slow cross-head speeds (1 mm/min) and maintenance of the a/b ratio at 0.4 was expected to produce stable crack growth. The typical load-extension curve for a

quasi-static propagation in paper is shown in Figure 2.17b. The area under the curve has been taken as the work of fracture, R , which was, expressed as work of fracture per unit fracture length.

Figure 2.18 shows the comparison between critical strain energy release rate and work of fracture for eight different papers. Although the two techniques of measuring G_c and R are distinctly different, it has been shown that these values are theoretically identical for linear elastic materials (Gurney and Hunt 1967).

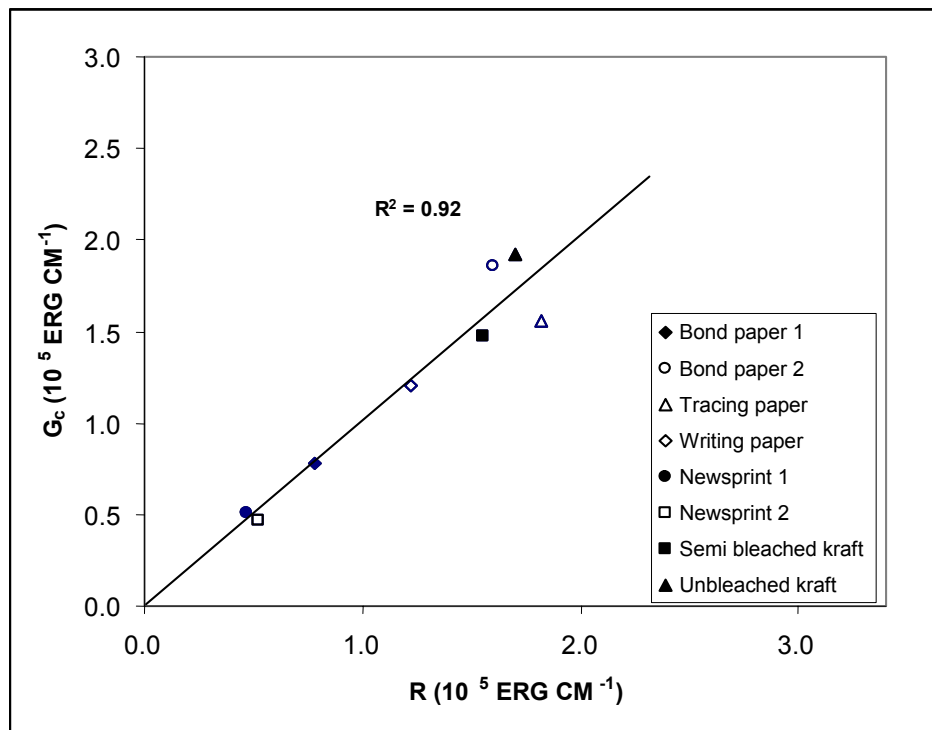


Figure 2.18 The comparison between critical strain energy release rate (G_c) and work of fracture (R) obtained from quasi-static fracture technique (Seth and Page 1974)

The data in Figure 2.18 suggests a very good agreement between G_c and R for most of the samples. This indicates that most of the tested samples are behaving as linear elastic materials. The MD elongation-to-break (%) data of these samples confirms that most of these samples were brittle. However, tracing paper and bond paper 2 were showing greater elongation-to-break (%) than other samples indicating these may not behave as linear elastic materials but have seen accompanying some plastic deformation. It appears from the figure that the data that deviate from the linearity were the data from samples that may show plastic deformation.

Seth and Page (1974) also reviewed similar work carried out by Balodis (1963) and Andersson and Falk (1966) and compared their results with these shown in Figure 2.18. Balodis investigated various kraft papers made from pulp with different beating levels. He measured the strain energy release rate using the Griffith-Irwin relations (equations 2.6 & 2.10) without considering the correction for the plastic deformation. However the G_c values obtained by Balodis were less than 10% of those obtained by Seth and Page. The G_c values obtained by Andersson and Falk were less than 20% of Seth and Page. Seth and Page suggested that the reason for low values of G_c for both Andersson and Falk's and Balodis's measurements was due to sample dimensions. Seth and Page claimed that G_c can only be measured accurately on sufficiently wide samples with long crack length. This was claimed to eliminate any influence of the specimen boundaries on the crack-tip stress distribution and to ensure that the net stress over the uncracked region of the sample remains less than yield stress.

2.8.2.3 Cohesive softening approach

Following conditions similar to the quasi-static and Goldschmidt and Wahren's (1968) approach, Tryding and Gustafsson (2000) described a way of estimating fracture properties of paper using a relatively short span un-notched specimen. They claimed that cohesive crack type approach is useful for paper because the size of the fracture process zone (FPZ) (see details in section 2.9.3.1) in paper is generally not small when compared to the size of the defects that start the fracture.

One important step in this method is that the failure should be stable and controlled. Their method is based on the idea that when failure starts, the deformation is no longer uniform along the specimen and then the specimen separates into two parts. The two parts are the localised fracture region and outside the fracture region. As the elongation continues the deformation and damage in the fracture region continue to increase although the load is now falling. The rest of the sample now experiences the unloading and hence the strain decreases with decreasing load. Figure 2.19 (A) shows the stress-strain curve obtained from a short un-notched specimen. Part B in the figure shows the total elongation of the specimen (δ) after the peak load. Tryding and Gustafsson used two curves to characterise the paper samples using their cohesive softening approach,

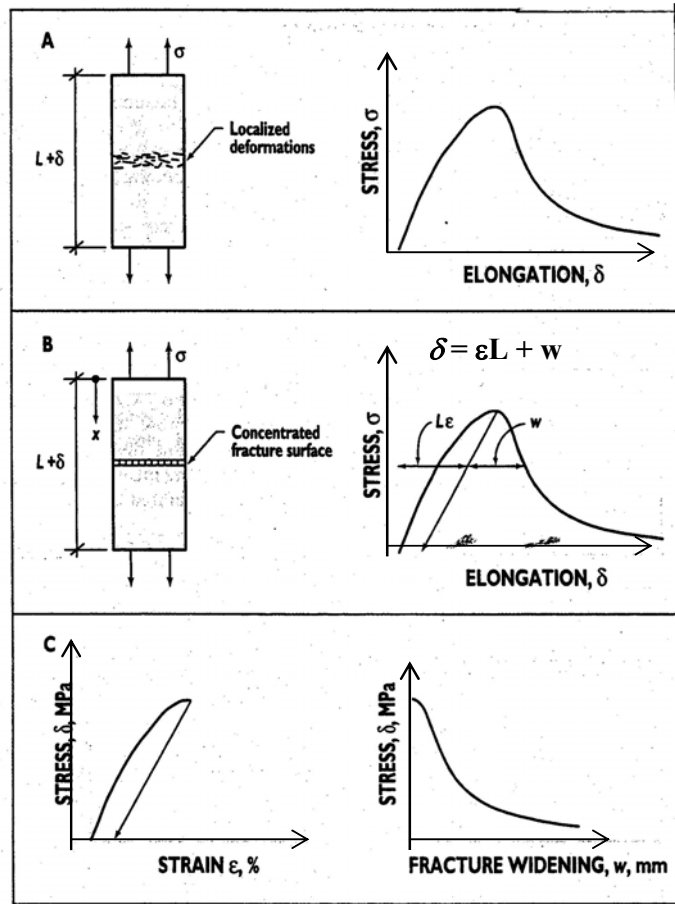


Figure 2.19 Stress-strain curves obtained from short and stable crack growth using a quasi-static approach (Tryding and Gustafsson 2000)

where one curve gives the performance of the material outside the fracture zone during loading and unloading and the other gives the performance of the material in the fracture region, as shown in the part C of the figure. The fracture energy (G_f) was calculated from the area under the load – fracture widening curve and then normalised by the width and thickness of the sample. Tryding and Gustafsson (2001) extended the cohesive crack approach to analyse notched newsprints in mode I failure. They reported that this method predicts the final failure of the sheet, independent of the sheet size and the initial crack length. Tryding and Gustafsson's cohesive softening method is easy to perform provided the testing equipment is stiff. The initial work using this method has shown some promising results. One problem with this method is the need for two separate tests to obtain the fracture energy. One test is required to obtain the strain before the peak stress and the other to obtain the fracture widening strain. The

technique appears to be promising, but further testing of this method is required before it can be considered as an established technique.

2.8.2.4 Summary

The application of LEFM techniques on various types of papers has confirmed that the use of laboratory sized specimens to measure the strain energy release rate or intrinsic fracture toughness is successful only for brittle papers such as newsprint. Specimens of at least 50 cm width are required to obtain a sample geometry independent value of G_c for tough, ductile papers. The major problem with application of LEFM to paper is that most papers are not linearly elastic but are instead elastic-plastic materials showing significant plastic deformation. Therefore attention has focused on the application of non-linear fracture mechanics to characterise fracture toughness.

2.9 Non-linear fracture mechanics

It is generally known that the crack-tip, stress or strain field cannot be characterized by a single parameter, such as the failure stress, when the yielding in the crack-tip region becomes extensive. If the paper specimen is large, a crack is reasonably long and the paper is significantly brittle, then paper may yield just in the crack tip area. However, when the sample is small, the crack is short and paper is ductile then the plastic deformation will spread into a larger area of the specimen. The energy consumed in the region where fracture process occurs is the only energy associated with fracture toughness. Therefore it is important to understand characteristics of the region where fracture processes occur.

2.9.1 Fracture Process Zone (FPZ)

When a specimen with a crack is subjected to in-plane stress, microscopic level damage (rupture of fibre-fibre bonds and deformation and fracture of fibres) occurs in a region just ahead of the crack tip. The fracture process always takes place in this small region, regardless of the size of the structure that fails through fracture. In any material, an important process in this region is the nucleation and growth of micro-separations, which eventually merge into a single body with the main crack (Broberg 1999). It is well established that the fracture energy is related to the size of the microscopic damaged area (Kettunen and Niskanen 2000). Seth et al (1993) reported that the area along the fracture line of a paper can be separated into two parts. The localised region, where actual failure and fracture energy consumption occurs is called the Fracture

Process Zone (FPZ) and the region where non-essential energy is dissipated for plastic deformation is called outer plastic zone.

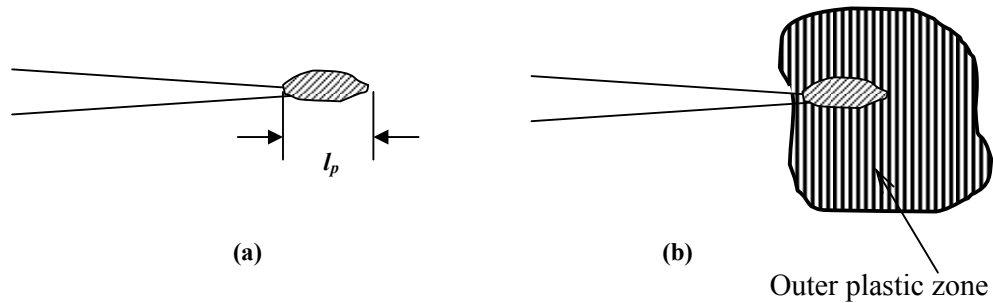


Figure 2.20 (a) Fracture Process Zone (FPZ) of an elastic material (b) FPZ and outer plastic zone of an elastic-plastic material (Mai 1988)

Figure 2.20 shows the FPZ of an elastic material and an elastic-plastic material. The size and shape of outer plastic zone is dependent on specimen and crack geometry and loading configuration. Application of non-linear fracture techniques to paper essentially attempts to characterise the energy consumed in the FPZ alone.

2.9.2 *Developments in non-linear fracture measurement techniques*

Although non-linear fracture techniques have been widely applied for different materials, direct application of the techniques to paper has not always been possible. Proposals were made to use the amount of crack opening prior to crack extension as a parameter, which could be treated as an intrinsic property of the crack-tip region in paper (Cotterell and Reddel 1977; Tanaka and Yamauchi 1999). The crack opening displacement (COD) at the crack-tip is commonly called the “Crack Tip Opening Displacement” or CTOD. The CTOD reaches a critical value at the onset of crack propagation and this has been used as a characteristic value of a material’s fracture resistance. Steadman and Sloane (1990) applied this technique to paper by observing the crack tip using a video camera. In this study, the critical CTOD values of sack paper and newsprint were compared. Although they concluded that this method is a useful technique to estimate fracture resistance of paper, the critical CTOD values were not obtained from right at the crack tip but rather from close to the crack tip. Tanaka and Yamauchi (1999) proposed a new method of measuring the COD by capturing images on a dot-printed double notched specimen under load using a video-microscope. They identified three deformation processes while the sample was under load. These

were elastic deformation process, plastic deformation process without crack propagation and further plastic deformation process with crack propagation as shown in Figure 2.21.

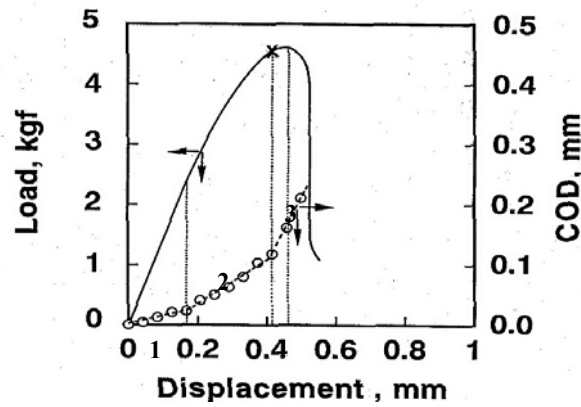


Figure 2.21 Load-displacement curve of a double-notched sample and COD-displacement relationship obtained for unbleached sack kraft. The x mark on the load-displacement curve shows the estimated onset of crack propagation (Tanaka 1998).

The measurement of spatial extent of microscopic damage zone along the crack line in paper was also attempted as a way to characterize the fracture energy (Kettunen and Niskanen 2000; Kettunen, Yu et al. 2000). The idea behind this method was that a wider

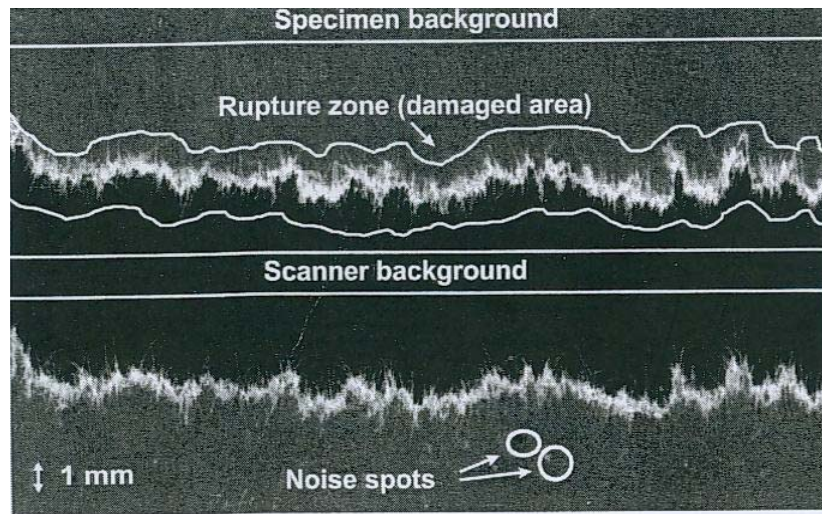


Figure 2.22 Scanned image of the fractured sample after a tear test (Kettunen and Niskanen 2000)

damage area means that more fibres are pulled out and less are broken. Figure 2.22 shows the image of a fractured newsprint sample tested along the MD direction in an in-

plane tear test. A silicone impregnation technique (Korteoja, Lukkarinen *et al.* 1996) was used to observe the broken inter-fibre bonds and fibres along the fracture line. However, there is no simple relationship between the width of the damage zone and the fracture energy.

The path independent J-integral, Liebowitz non-linear technique and Essential Work of Fracture (EWF) methods are other successful alternative non-linear techniques that have been used in the evaluation of the fracture toughness of paper. The details of these techniques are given in the next sections.

2.9.3 The J Integral method

Rice (Rice 1968) proposed the J-integral technique as a method for characterizing the stress-strain singularity at the crack tip. Rice showed that a particular line integral taken

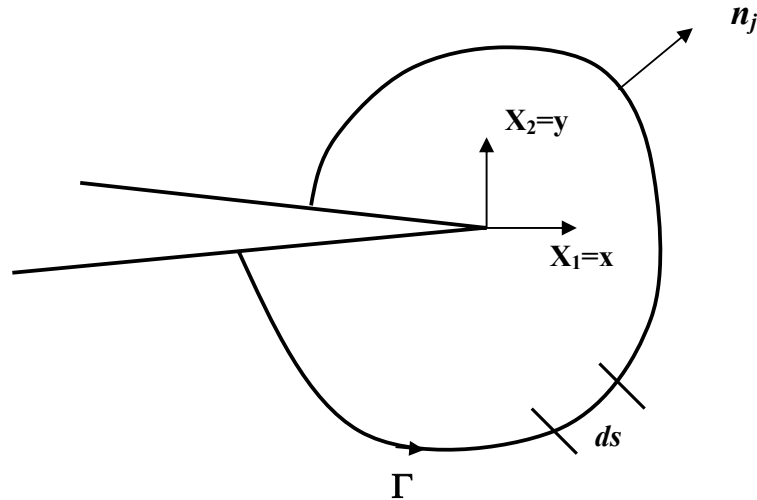


Figure 2.23 The integration path Γ for the determination of J for a 2-D body

around the crack tip is independent of the integration path, Γ . Generally, for a homogeneous, linear or non linear elastic material (subjected to a two-dimensional, (x, y) deformation field), the line integral J, on any curve starting from the lower surface

and ending on the upper surface surrounding the crack tip (see Figure 2.23), is defined by the following equation:

$$\mathbf{J} = \int_{\Gamma} [Wdy - \mathbf{T} \frac{\partial \mathbf{u}}{\partial x} ds] \quad 2.12$$

Here W is the strain energy density ($\partial W / \partial \varepsilon_{ij} = \sigma_{ij}$), \mathbf{T} is the traction vector on Γ , $T_i = \sigma_{ij} n_j$ according to an outward unit vector \mathbf{n} (with direction cosines n_j), \mathbf{u} is the displacement vector and ds is an element arc length along Γ .

The J integral, which can be interpreted as the rate of change of potential energy per unit crack length (Rice 1968; Begley and Landes 1972) has been used as a more general way of evaluating J experimentally. This relationship is given by,

$$\mathbf{J} = -\frac{dU}{da} = \int_0^{\delta} \left(-\frac{\partial P}{\partial a} \right)_{\delta} d\delta = \int_0^P \left(\frac{\partial \delta}{\partial a} \right)_{P} dP \quad 2.13$$

where U is the potential energy per unit thickness, a is the crack length, P is the load per unit thickness and δ is displacement. For an elastic material, U is the area under a load-elongation curve and represents the energy consumed for crack propagation. However, for large-scale yielding, elastic-plastic materials like paper, U is the work done in deforming the specimen but does not simply represent the energy consumed for crack propagation.

In the application of the J-integral technique, two basic methods, one with multiple specimen sizes (Begley and Landes 1972) and the other with a single specimen size (Rice, Paris *et al.* 1973) have been applied.

2.9.3.1 Multiple-specimen method

A typical outline of this approach is shown in Figure 2.24 (Yuhara and Kortschot 1993).

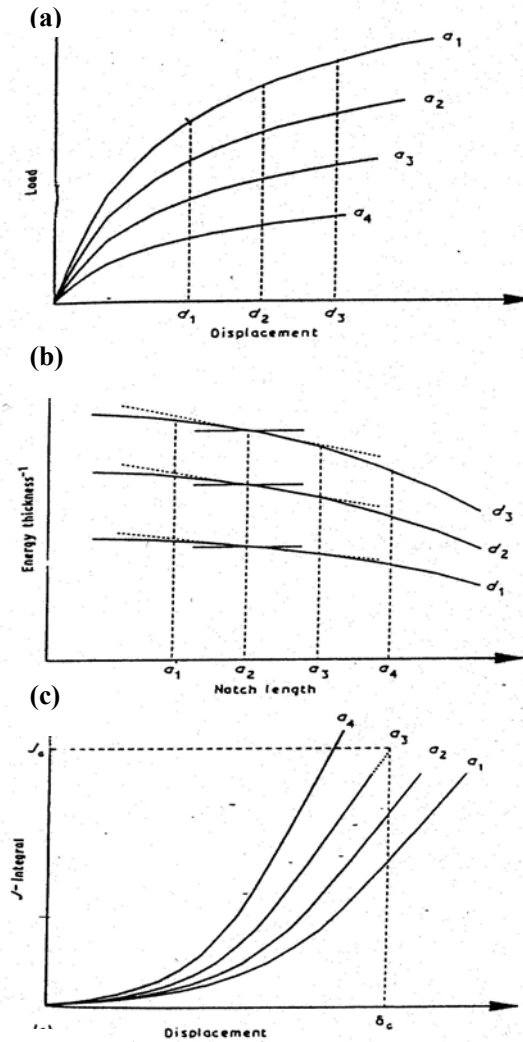


Figure 2.24 Typical graphical analysis of multiple specimen method (Yuhara and Kortschot 1993)

As a first step, the load-displacement curves for a series of notched specimens with different crack length are obtained (see Figure 2.24a). The work done up to a certain displacement is obtained for each crack length using the load-displacement curves and the energy versus crack-length curves are obtained for each displacement. The gradients of these curves can be then interpreted as the J-integral (Figure 2.24b). The gradient divided by the sheet thickness has been defined as the J-integral value for each displacement. Finally by plotting the curves of J-integral values versus displacement, the critical value of the J-integral can be estimated using the displacement at which the onset of crack growth occurs, as shown in Figure 2.24c. This critical value is then taken as the fracture toughness.

It is necessary to have at least three specimens with different crack lengths to obtain the J-integral value using the multiple-specimen technique. However, for a non-uniform material like paper, large numbers of test specimens are required to obtain reliable load-displacement curves. Additional time is also required for graphical interpretation and analysis, making use of the multiple-specimen technique unreasonable for routine measurements.

2.9.3.2 *Single specimen or R.P.M. method*

To overcome the problems associated with the multiple specimen method Rice, Paris and Merkel (Rice, Paris et al. 1973), developed a single specimen technique which gives only one critical J (J_c) value. Rice, Paris and Merkle (R.P.M) proposed a technique to determine the J-integral using just one load-displacement diagram of a double-edge notched specimen. This method is derived on the basis of two main assumptions. The first assumption is that the total displacement, δ , is the sum of an elastic displacement (δ_c) and an irreversible plastic displacement (δ_p).

$$\delta = \delta_c + \delta_p \quad \mathbf{2.14}$$

The second assumption is that the plastic displacement can be expressed in the following form:

$$\delta_p = bh(P/b) \quad \mathbf{2.15}$$

where b is the ligament length, P is the applied load and h is a function of P/b that also includes material parameters such as elasticity (E), yield stress (σ_y) and strain-hardening coefficients (n).

After taking these assumptions into consideration, the J-integral can be written as the sum of elastic and plastic components.

$$J = J_e + J_p \quad \mathbf{2.16}$$

$$J = J_e + \int_0^P \left(\frac{-\partial \delta_p}{\partial b} \right) dP \quad \mathbf{2.17}$$

Rice *et al*, (1973) then derived the following expression for the J integral from an elastic-plastic analysis,

$$J = J_e + \frac{1}{b} \left(2 \left[\int_0^{\delta_p} P d\delta_p - \frac{1}{2} P \delta_p \right] \right) \quad 2.18$$

Here J_e has been described as strain energy release rate, G , and for an orthotropic material is given by,

$$J_e = G = \frac{K^2}{E} \quad 2.19$$

Equations 2.18 and 2.19 give

$$J = G + \frac{2}{b} \left[\int_0^{\delta_p} P d\delta_p - \frac{1}{2} P \delta_p \right] \quad 2.20$$

The term in the bracket, which is associated with the plastic component, can be directly determined from the shaded area of the load-displacement curve shown in Figure 2.25.

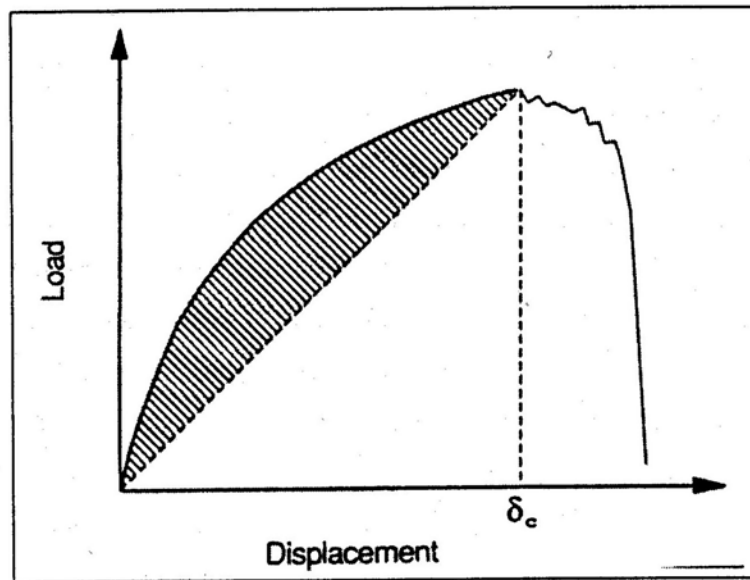


Figure 2.25 Load-displacement diagram of a double notched specimen (Yuhara and Kortschot 1993)

The modulus of the material (which is required to calculate the elastic component) must be measured using an unnotched specimen. Thus this method requires only measuring one set of notched and one set of unnotched specimens, and requires less experimental effort and analysis than the multiple-specimen technique.

2.9.4 Liebowitz non-linear technique (LNT)

Liebowitz non-linear technique (LNT) is another method used to estimate fracture toughness of paper. LNT has gained some recognition as a reliable non-linear method to estimate fracture toughness. Liebowitz and Eftis (1971) formulated a non-linear fracture toughness parameter, G_c from a Ramberg - Osgood type description (which draws two secant moduli $\alpha_1 M$ and $\alpha_2 M$ to the load-displacement curve) of a non-linear load-elongation (P - δ) curve. In the LNT method, load (P) and displacement (δ) are related by the equation;

$$\delta = \frac{P}{M} + k \left(\frac{P}{M} \right)^n \quad 2.21$$

where $k (\geq 0)$ and $n (\leq 1)$ are parameters characterizing the deviation from linearity and M is the initial stiffness of the centre notched specimen. Two points (P_1, δ_1) and (P_c, δ_c) (see Figure 2.26) are selected on the non-linear part of the load-displacement curve and

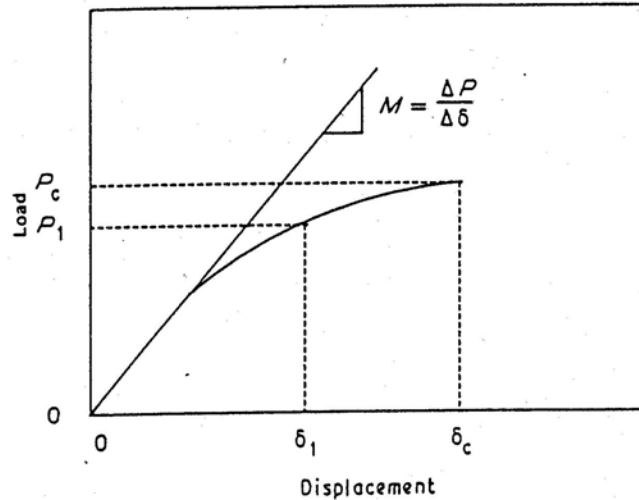


Figure 2.26 Selection of two points (P_c, δ_c) and (P_1, δ_1) from non-linear part of a typical load-elongation curve for a centre notched specimen (Westerlind, Carlsson *et al.* 1991)

these values are substituted into equation (2.21) to obtain the parameters, k and n . A non-linear correction factor β was introduced to the elastic energy release rate (G) and the following expression was obtained,

$$\mathbf{J} \approx \tilde{G} = (1 + \beta) \mathbf{J}_e \quad 2.22$$

where J_e is the elastic component of the J-integral. At the critical point, $P = P_c$ and $J = J_c$ and β can be shown to be

$$\beta = \frac{2nk}{n+1} \left(\frac{P_c}{M} \right)^{n-1} \quad 2.23$$

$$J_c \approx \tilde{G} = \left\{ 1 + \frac{2nk}{n+1} \left(\frac{P_c}{M} \right)^{n-1} \right\} \quad 2.24$$

Using equation (2.24), the specific fracture energy J_c/ρ , (where ρ is sheet density) can be obtained.

2.9.5 Application of Liebowitz and J-integral techniques

Westerlind *et al*, compared the fracture toughness of linerboard obtained using the Liebowitz technique, and the single and multiple specimen J-integral methods.

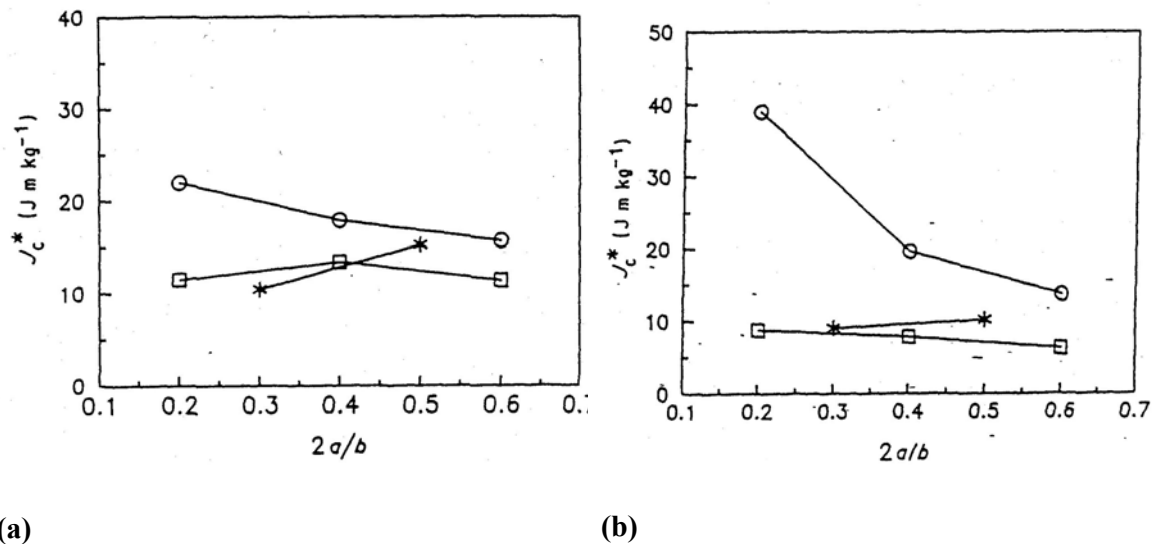


Figure 2.27 Specific fracture toughness against crack length to width ratio ($2a/b$) for 200 gsm kraft linear (a) MD & (b) CD obtained from three different techniques. (The symbols are: *Star* – Multiple-specimen, *Circle*- Single specimen and *Square*- Liebowitz method)

They essentially compared the accuracy and convenience of these methods in the determination of fracture toughness. For these fracture measurements a universal tensile tester at a cross head speed of 1 cm/min was used. As the centre of the notched specimens tended to buckle out of plane around the crack, buckling supports were fitted into the testing rig. Kraft liner samples with two different grammages (200 g/m^2 and

400 g/m²) were selected for the tests. Machine direction (MD) and cross direction (CD) test pieces prepared from each sample (grammage) were tested using J-integral multiple and single specimen methods and the Liebowitz method. The results obtained from the tests carried out on 200 g/m² kraft liner are shown in Figure 2.27.

In this data, it can be seen that measurements made using the single specimen technique always gave larger values than those obtained using the multiple-specimen and Liebowitz methods. It was found that the values obtained from multiple specimen method were independent of crack length, while the values obtained from the single specimen method were strongly dependent on crack-length. The results obtained from the multiple-specimen and Liebowitz methods also gave reasonably similar fracture toughness values. The major drawback in multiple specimen method is that it is a time consuming technique and requires large numbers of sample, so it is impractical for routine testing. Westerlind *et al.* (1991) recommended the Liebowitz method as a better method, in terms of convenience, to measure fracture toughness.

Other studies comparing the single and multiple specimen methods showed that the measured toughness values were comparable for brittle filter papers. However, there have been many other reports of disagreements (similar to the Westerlind *et al* study) between the results obtained from the two techniques for tough ductile papers (Steadman and Fellers 1986; Pouyet, Volozinskis *et al.* 1989; Yuhara and Kortschot 1993).

Yuhara and Kortschot (1993) reported that the single specimen technique overestimates the value of J_c compared with the multiple specimen technique. It was also found that single specimen values were substantially dependent on sample geometry (Steadman and Fellers 1986). One of the assumptions made in the single specimen technique is that the plastic displacement of a specimen with a deep notch is only a function of the load per unit length of the ligament (equation 2.15), although under some circumstances this assumption is invalid. Yuhara and Kortschot (1993) proposed a formula to overcome the dependence of J_c on sample geometry. The generalized formula is given by,

$$\delta_p = bh(P/b^m) \qquad \qquad \qquad 2.25$$

By using $m=0.8$ they reported that the results obtain from the modified equation and the multiple specimen method were then comparable.

Another shortcoming of the single specimen technique is that the critical load at the onset of crack propagation is required before J_c can be determined. This is extremely difficult for a material like paper (Kazi and Kortschot 1996), since there is no unique definition of the point where the crack growth initiates (Wellmar, Fellers et al. 1997). In most calculations the maximum load is taken as the critical load, which is not always true (Tanaka, Otsuka et al. 1997; Wellmar, Fellers et al. 1997). Therefore the estimation of J_c for paper using the single-specimen method is questionable.

Swinehart and Broek (1995) obtained an expression for the strain energy release rate (J) without an integral. They claimed that LEFM based stress intensity factor calculations to characterise fracture toughness are better than the method based on the J-integral. The main grounds for opposing the use of the J-integral were given as (i) The J-integral assumption that the stress – strain curve is non-linear elastic (ii) J_c increases as the fracture is still in progress (iii) poor agreement between measured and calculated values (iv) material performances cannot be ranked just on the knowledge of J_c alone as the stress-strain curve must also be taken into account.

Wien and Gottsching (1999) also questioned the use of J-integral for the characterisation of fracture toughness of a material that exhibits significant amount of plastic deformation at the crack tip. They claimed that in such a situation fracture toughness depends on the specimen geometry.

Fellers *et al* (1992) investigated a production problem of cracking of corrugated boards during die cutting using J – integral and Liebowitz methods. They compared the values obtained from J-integral with the “die-cutting toughness number”, a property defined as the cracking resistance of the corrugated board during die cutting and they found an excellent correlation between the J-integral and the die-cutting toughness number. However, Liebowitz method also used in this study showed a higher precision than the J-integral technique.

A test method based on the Liebowitz technique and J-integral to measure fracture toughness was proposed by the researchers at the Swedish pulp and paper research institute (STFI) (Wellmar, Fellers et al. 1997). An instrument was also developed based on this method to measure fracture toughness of paper (Fellers 1995; Fellers 1996). Since this method has been added as a SCAN-test standard (SCAN-P77:95:1995), examining the theory behind this method and its implementation in the L & W instrument is important.

2.9.5.1 Theory behind STFI method

A constitutive equation was derived to describe the mechanical behaviour of an elastic, strain-hardening solid based on deformation theory of plasticity (details are given in (Wellmar, Fellers et al. 1997)) as follows:

$$\varepsilon_{ij} = C_{ijkl}^{-1} \sigma_{kl} + \frac{3}{2} \left(\frac{\sigma_e}{E_o} \right)^n \frac{S_{ij}}{\sigma_e} \quad 2.26$$

where ε_{ij} and σ_{ij} are the strain and stress tensors respectively. C_{ijkl}^{-1} is the inverse of the 4th order tensor of elastic moduli. E_o is the initial generalised modulus and n is the hardening exponent. S_{ij} and σ_e are the components of the stress deviator and the effective (Von Mises) stress, respectively. E_o and n are obtainable from a uniaxial tensile test performed on the material. In the special case of uniaxial tension the equation 2.26 reduces to Ramberg-Osgood form.

$$\varepsilon_2 = \frac{\sigma_2}{E_2} + \left(\frac{\sigma_2}{E_0} \right)^n \quad 2.27$$

Now the parameters ε_2 , σ_2 and E_2 are the strain, stress and elastic modulus, respectively, in the direction perpendicular to the crack. When the tensile test is carried on a flaw free test piece, the sample load-elongation obtained from the test can be fitted with the following equation:

$$\delta = \frac{F}{c} + k \left(\frac{F}{c} \right)^n \quad 2.28$$

Here δ is the elongation, F is the measured force and c (stiffness) specifies the tangent to the load-elongation curve at the origin. The parameters k and n are determinable from a tensile test. Equations (2.27) & (2.28) are related each other by:

$$\left(\frac{E_2}{E_o}\right)^n = kl^{n-1} \quad 2.29$$

$$\varepsilon_2 = \frac{\delta}{l}, \sigma_2 = \frac{F}{A_o}, E_2 = \frac{c.l}{A_o} \quad 2.30$$

where l and A_o are the length and the cross sectional area of the tensile test piece. Then expressions for $n (\geq 1)$ and $k \geq (0)$ can be obtained by solving the equation (2.28), using the condition $\delta(F_N) = \delta_N$ and from the work (U) under the tensile load-elongation curve. Here δ_N is the elongation at the failure load (F_N). The expressions for n and k are:

$$n = \frac{F_N \left(\frac{F_N}{c} - \delta_N \right)}{U - F_N \delta_N + \frac{F_N^2}{2c}} - 1 \quad 2.31$$

$$k = \frac{\delta_N - \frac{F_N}{c}}{\left(\frac{F_N}{c} \right)^n} \quad 2.32$$

Now consider elongation of a centre notched test piece with span $2h$, width $2W$ and crack length $2a$ as shown in Figure 2.28.

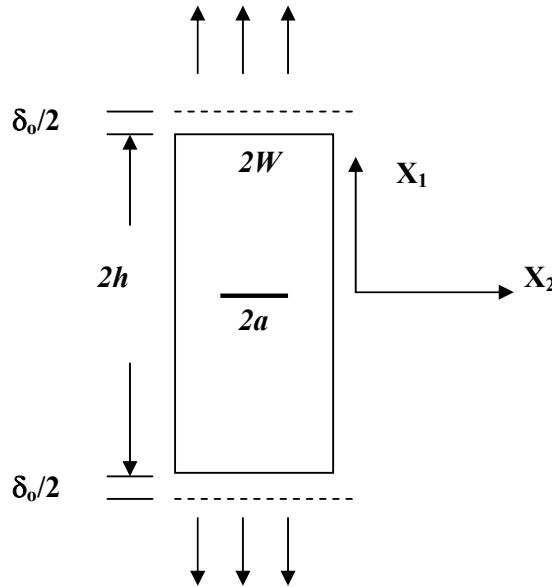


Figure 2.28 Centre notched test configuration used in the STFI J-integral method

Using the fracture criterion based on J-integral, as expressed in equation 2.12 and applying the test configuration in Figure 2.28, an expression is derived for J using material parameters as follows (Wellmar, Fellers et al. 1997):

$$J = \frac{h(1-\nu_{12}\nu_{21})}{E_2} \sigma_2^2 f_1 + \frac{2hn}{n+1} \phi \sigma_o \varepsilon_o^n \left(\frac{\sigma_2}{\sigma_o} \right)^{n+1} f_2 \quad 2.33$$

here ν_{12} and ν_{21} are Poisson's ratios, which from symmetry are related to each other by:

$$\nu_{12}E_2 = \nu_{21}E_1 \quad 2.34$$

where E_1 and E_2 are the elastic moduli in X_1 and X_2 directions respectively. Here f_1 and f_2 are geometrical factors which need to be obtained using Finite Element Method (FEM). For the test configuration shown in Figure 2.26 f_1 and f_2 were empirically determined as:

$$f_1 = 0.5617 (E_1/E_2)^{-0.1899} \quad f_2 = 0.5 + 0.512 \tanh(0.206n) \quad 2.35$$

In Equation 2.34, σ_o is the reference stress value that is set to the yield strength and related to the reference strain ε_o through

$$\varepsilon_o = \sigma_o \left(\frac{1-\nu_{12}\nu_{21}}{E_2} \right) \quad 2.36$$

and

$$\phi = \frac{kl^{n-1} (2-\nu_{12})(\nu_{12}^2 - \nu_{12} + 1)^{\frac{n-1}{2}}}{2(1-\nu_{12}\nu_{21})^n} \quad 2.37$$

Since the elongation, δ_o can be obtained from the load-elongation curve of the notched specimen, the σ_2 term in the equation 2.28 can be determined by numerically inverting the stress-strain relation of a cracked structure given by:

$$\varepsilon_2 = \frac{1-\nu_{12}\nu_{21}}{E_2} \sigma_2 + \left(\frac{1-\nu_{12}\nu_{21}}{E_2} \sigma_2 \right)^n \phi \quad 2.38$$

The Poisson's ratios are calculated from combining equation (2.34) with the approximation that $\nu_{12}\nu_{21} = (0.293)^2$ (Baum, Brennan *et al.* 1981). Now substituting the material parameters (F_N , δ_N , c , U , n and k) into equation 2.33, a plot of J vs elongation (δ_o) can be obtained as shown in Figure 2.29.

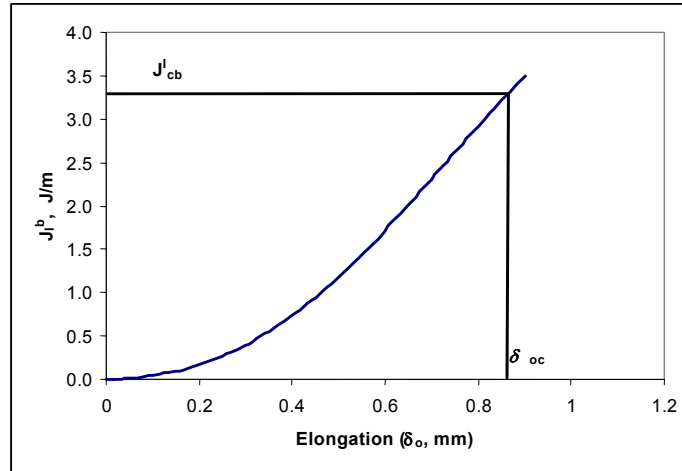


Figure 2.29 A plot of J_I^b ($= J_{I,t}$, where t is the thickness) against δ_o for the center notched test piece with $a/W=0.5$

For mode I fracture the crack growth occurs if $J_I \geq J_c$. After obtaining the critical displacement (δ_{oc}) at maximum load of the notched specimen, the corresponding critical point of crack growth initiation or J_c was obtained from the plot of J vs elongation as shown in Figure 2.27. Following the notations specified in ASTM standard, fracture toughness is defined as J_{Ic}^b ($J_c.t$) and the fracture toughness index is defined as $(J_{Ic}^w = (J_c.t)/w$, where t and w are the thickness and grammage (g/m^2) of the specimen.

2.9.5.2 Application of STFI J-integral method to measure fracture toughness

It is apparent from the theory on STFI J-integral method that application of this method to determine fracture toughness of paper requires measurements with ordinary crack free tensile test pieces as well as measurements with notched specimens. The tensile tests are carried out along both the MD and CD directions according to SCAN test standard (SCAN – P67:93 1993) on 100 mm span samples. The test pieces for the fracture toughness are prepared with dimensions that are usually 100 mm long ($2h$) and 50 mm wide ($2W$) to give $h/W = 2$ and relative crack length $0.1 < a/W < 0.7$. The load – elongation curve of the tensile test is analysed using a computer program to calculate the constitutive parameters. The tensile tests are carried out on 12 test pieces for each test and the fracture test is carried out on 6 to 10 notched test pieces for each test and the critical elongation at fracture is determined. The geometric factors f_1 and f_2 are empirically determined for the centre notched sample configuration.

The "L&W tensile tester with fracture toughness" is a tensile test equipment developed by STFI and Lorentzen & Wettre, for both notched and un-notched material testing to determine fracture toughness based on the STFI J-integral technique. The L&W tester is computerised and the attached software deals with the calculation of the material J-integral toughness.

In a recent work Wellmar *et al* (2000) reported the use of STFI J-integral criterion to predict fracture initiation in large structures, based on a standard test performed on small laboratory specimens. Tests were carried out on both newsprint and sack paper. The test pieces used in the tests had dimensions 1000 mm x 500 mm (span x width), which is much larger than standard tensile test pieces. They reported that fracture initiation in paper structures could be predicted with this method in terms of either critical force or critical elongation. Fellers *et al* (2001) investigated the effect of reinforcement pulp characteristics in TMP papers using fracture mechanics. The fracture toughness of these materials was determined by SCAN test method (SCAN-P77: 95 1995). They reported that fracture properties of TMP papers deteriorated with increased defect size but improved with small increase in the fraction of chemical pulp.

Although an instrument is available to measure fracture toughness using the J-integral method, the need for testing both notched and un-notched specimens to predict the fracture toughness makes STFI J-integral technique more cumbersome than would normally be expected from a QC technique. Another problem in this technique is the use in the calculation of maximum load as the critical load where the fracture initiates. This is correct for more brittle papers such as newsprint, but can introduce errors for some papers, where the crack only begins to propagate well after the maximum load has been reached (Wellmar, Fellers et al. 1997).

2.9.6 Essential work of fracture technique (EWF)

The concept of the essential work of fracture was first suggested by Broberg (1968; 1971; 1975), as a means of formulating a unified theory to describe fracture at both small-scale and large-scale yielding. Cotterell, Reddell, Mai and co-workers (1977; 1986; 1988; 1991; 1993) later developed the essential work of fracture technique, a method of separating the essential and non-essential energy consumed during fracture. This method has been identified as a simple and practical way of measuring the plane

stress fracture toughness of ductile polymers, thin films, sheets and toughened composite materials independent of specimen or crack geometry and using laboratory size specimens (Seth, Robertson et al. 1993; Mouzakis, Gahleitner et al. 1998; Mouzakis, Karger-Kocsis et al. 2000; Ferrer-Balas, MasPOCH et al. 2001; Lauke and Schuller 2001).

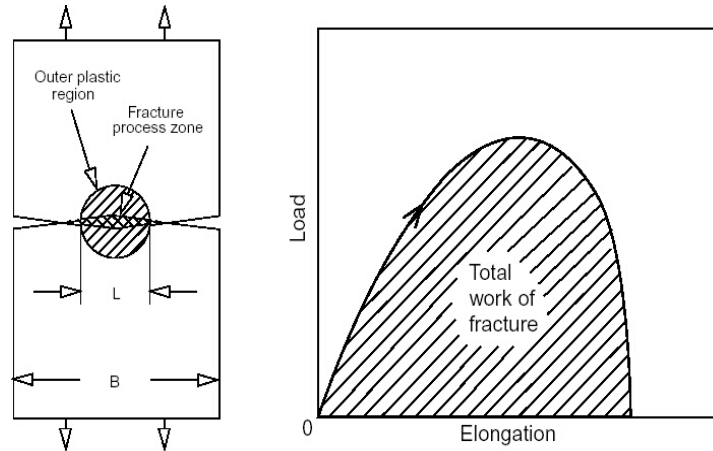


Figure 2.30 Schematic load-elongation curve (right diagram) of a DENT (left diagram) specimen. The shaded areas in the DENT specimen show the regions of energy dissipation in the measurement (Seth 1995).

When a tough elastic-plastic material with low yield stress is strained, the material yields not only in the FPZ but a significant amount of yielding can also occur well away from the FPZ. The extended irreversible deformation away from the FPZ generally depends on the specimen geometry and the toughness of the material and hence is not a material constant. The energy consumed at the crack tip in the FPZ is essential to the fracture while the energy consumed away from the crack tip is not essential. The work obtained from the load-elongation curve ($W = \int P du$) (see Figure 2.30) of a notched elastic-plastic material contains both essential and non-essential energy consumed during a fracture. For successful application of the essential work of fracture technique, it is necessary to use a suitable sample geometry that will allow the separation of the essential work from the total work of fracture. It has been shown that the Double Edged Notched Tension (DENT) geometry is the most suitable from the tested sample geometries (Cotterell 1977; Cotterell and Reddel 1977). Cotterell and Reddel assumed that if a DENT specimen (Figure 2.30) yields completely before fracture, the outer plastic region is almost circular and the diameter and the work in the outer plastic zone should be proportional to L^2 . In fact, the shape of the outer plastic zone can be circular,

elliptical or diamond shaped, provided that the area scales with L^2 . They noted that if the specific essential work w_e (the essential work per unit area of crack extension) remained constant then the essential work is proportional to L . The total work of fracture W_f can be then written as,

$$W_f = Lt w_e + \beta L^2 t w_p \quad \mathbf{2.39a}$$

where w_p is the specific non essential work, t is sample thickness and β is a shape factor for the outer plastic zone. For a circular zone $\beta = \pi/4$, while for an elliptical plastic zone $\beta = \pi h/4L$, where h is the height of the plastic zone. For an elliptical plastic zone, the h/L ratio must be constant if β is to be independent of the ligament length (Gdoutos 1993). Dividing both sides of the equation 2.39a by Lt yields,

$$w_f = W_f/Lt = (\beta w_p)L + w_e \quad \mathbf{2.39b}$$

This equation shows that the y-axis intercept determined from fitting a set of data of w_f versus L gives the specific essential work (w_e) of the specimen. It is necessary that the sample ligament completely yields before crack propagation in order for equation (2.39a) to be valid and also that the ligament remain in plane stress. The lower limit of the ligament length is controlled by the sheet thickness (t) and is of the order $L > 5t$. However in reality L should also be larger than the average floc size in the sheet (Seth 1995). The size of plastic region ahead of the crack tip determines the upper limit of the ligament length and in general it should not be larger than the size of the plastic region ($2r_p > L$). In order to avoid the interference with the crack tip stress distribution from the sample boundary, the specimen width (B) has to be set to $B/3 > L$. Equation (2.40) shows the expression for the radius of the plastic zone,

$$r_p = \frac{1}{2\pi} \left(\frac{K}{\sigma_{ys}} \right)^2 \quad \mathbf{2.40}$$

where K ($G = K^2/E$) is the stress intensity factor and σ_{ys} is the yield strength (Atkins and Mai 1988). Another important condition mentioned in the literature for successful application of EWF technique is the need for stable crack growth (Seth, Robertson *et al.* 1993; Yu and Karenlampi 1997). The argument is that, if the stored elastic energy at fracture is greater than the energy required for sample fracture then unstable fracture

can be occurring. If that is the case then sample fracture toughness can be overestimated. A few recommendations were made to achieve stable crack growth by Seth, Robertson *et al* (1993). These were the use of short specimens, stiff testing equipment and slow strain rates. As discussed in section 2.3.6, paper has no defined yield stress, and will yield under any load necessitating the practical definition of the yield stress as the stress where the strain first deviates by 0.2% from the initial slope of the data. However in practice significant amounts of energy will not be absorbed unless this yield stress is exceeded and so the statement that the ‘ligament should completely yield before the crack propagation’ remains generally applicable under this definition of yield stress.

2.9.6.1 Application of EWF method to paper

Several authors have studied the suitability and application of the essential work of fracture technique to paper (Seth, Robertson *et al*. 1993; Seth 1995; Tanaka, Otsuka *et al*. 1997; Yu and Karenlampi 1997; Karenlampi, Cichoracki *et al*. 1998; Tanaka 1998). Seth *et al* (1993) tested several commercial papers and laboratory handsheets made at different beating levels.

The calculation of the specific essential work of fracture requires the sample thickness. However the thickness of a heterogeneous, rough and porous material like paper varies significantly from one place to other in one single sample. Therefore Seth *et al*, (1993) replaced the thickness by sheet grammage (grams per unit area) g , to calculate a specific work of fracture $w_f (=W_f/Lg)$. In their work L/B was set to 0.3. Seth *et al* used a pair of line-type clamps mounted on a two guide rods to maintain uniform stress in the plane of the sheet. The reason for having linear guide rods is to ensure that the specimen is free from buckling and only loaded in plane. Seth later confirmed that the effect of buckling in DENT specimens of paper is insignificant (Seth 1995). However, the guide rods are useful, especially when loading tough wide samples, to ensure that the samples experience a tensile mode of fracture.

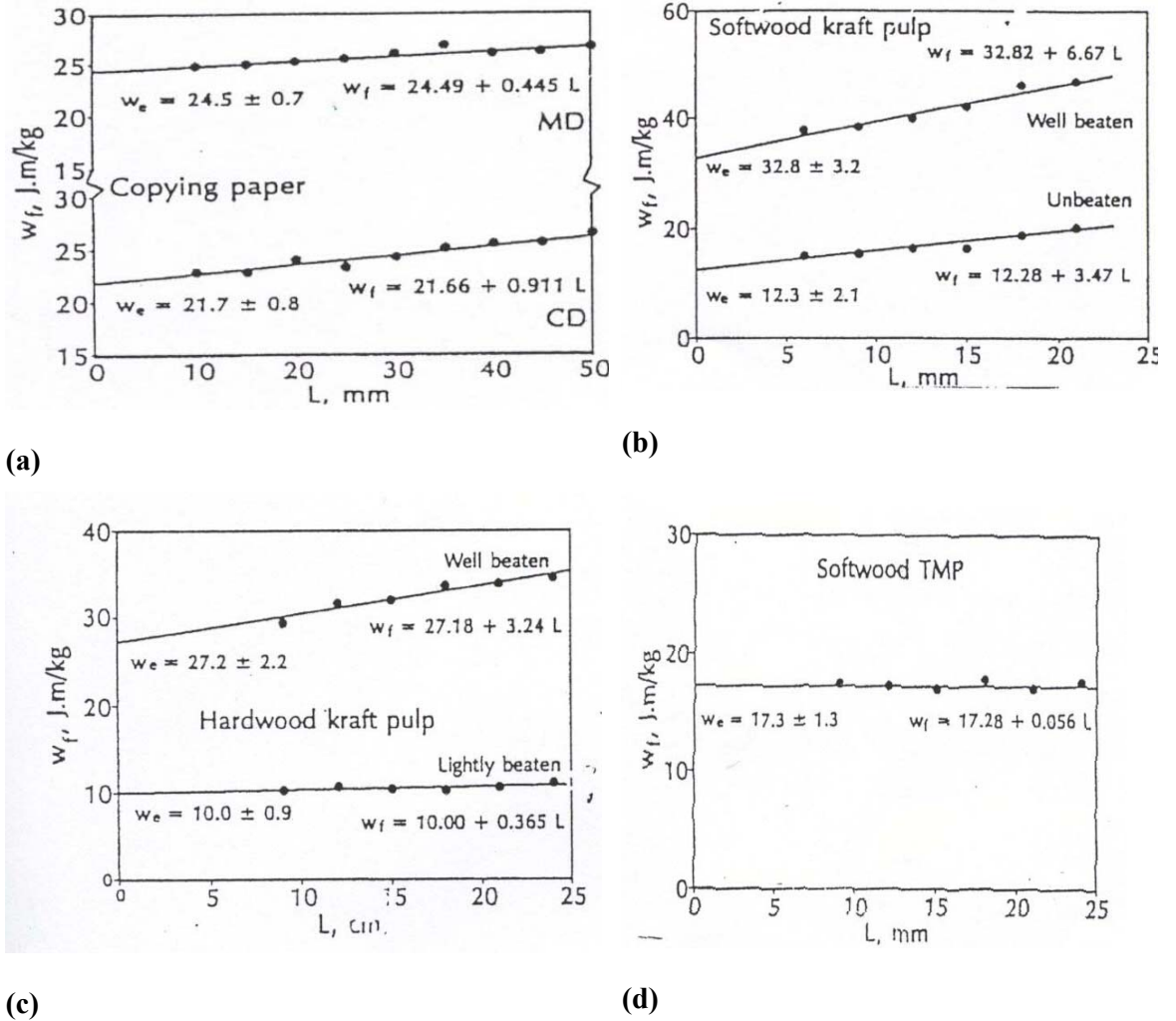


Figure 2.31 w_f against ligament length (L) for (a) copy paper (b) softwood kraft (c) hardwood kraft and (d) softwood TMP (Seth, Robertson *et al.* 1993)

Figure 2.32 shows the w_f against L plots obtained for different specimens. The w_e of the softwood and hardwood kraft pulps clearly increases with beating. The near zero slope with ligament length in the data obtained from TMP sheets indicate that the plastic deformation outside the FPZ is negligible for these samples.

2.9.6.2 The relationship between CTOD (Crack-Tip Opening Displacement) and EWF

Cotterell and Reddell (1977) attempted to relate the critical crack tip opening displacement (δ_c) and yield strength (σ_{ys}) to the essential work of fracture. If it is assumed that the maximum load P_{max} is reached before crack initiation, then P_{max} can be written as,

$$P_{\max} = \alpha Lt \quad 2.41$$

where α is a constant. If e_m is the ultimate elongation, an (approximate) expression for the work of fracture W_f is,

$$W_f = \xi P_{\max} e_m \quad 2.42$$

where ξ is a shape factor that depends on the shape of the load elongation curve. The work of fracture can be written as:

$$W_f = \xi \alpha Lt e_m = (Ltw_e + \beta L^2 tw_p) \quad 2.43$$

The ultimate elongation is given by,

$$e_m = (w_e + \beta Lw_p) / \alpha \xi \quad 2.44$$

Equation (2.44) gives a linear relationship between ultimate elongation and ligament length. The intercept at zero ligament length gives $w_e / \alpha \xi$. Assuming that the ligament is under plane stress, the ultimate elongation at zero ligament length would be the critical crack tip opening displacement (the surrounding plastic zone vanishes for a small ligament length). Hill (1952) defined the constant α as,

$$\alpha = \frac{2}{\sqrt{3}} \sigma_{ys} \quad 2.45$$

Assuming the shape of the load-elongation curve is parabolic, the shape factor ξ has been approximated as 2/3 (Hill 1952). Hence the specific essential work of fracture is given by:

$$w_e = 0.77 \sigma_{ys} \delta_c \quad 2.46$$

Seth et al (1993) and Seth (1995) also attempted to relate the fracture toughness estimated from the EWF method to that obtained from the crack tip opening displacement (CTOD). The elongation to fracture was plotted against the ligament length as described in equation (2.44). The intercept (ε_0) of this linear relationship has been defined as the critical crack tip opening displacement. Figure 2.32 illustrates a schematic of the stress and extension at the crack tip at the point of crack propagation.

When the crack tip opening displacement reaches the critical value, the stress at the crack tip is assumed to be either at the yield stress (σ_{ys}) or at a higher value.

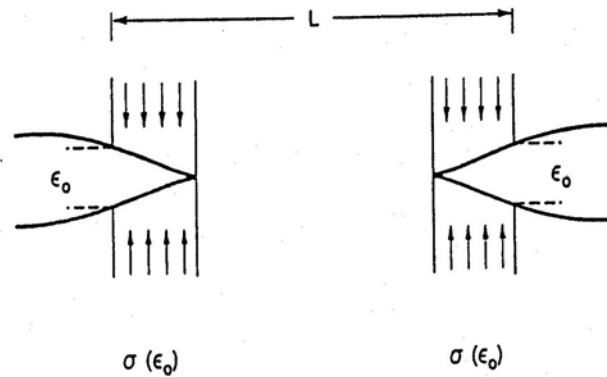


Figure 2.32 Stress and elongation of a DENT sample near crack tip at the initiation of crack growth (Seth, 1995)

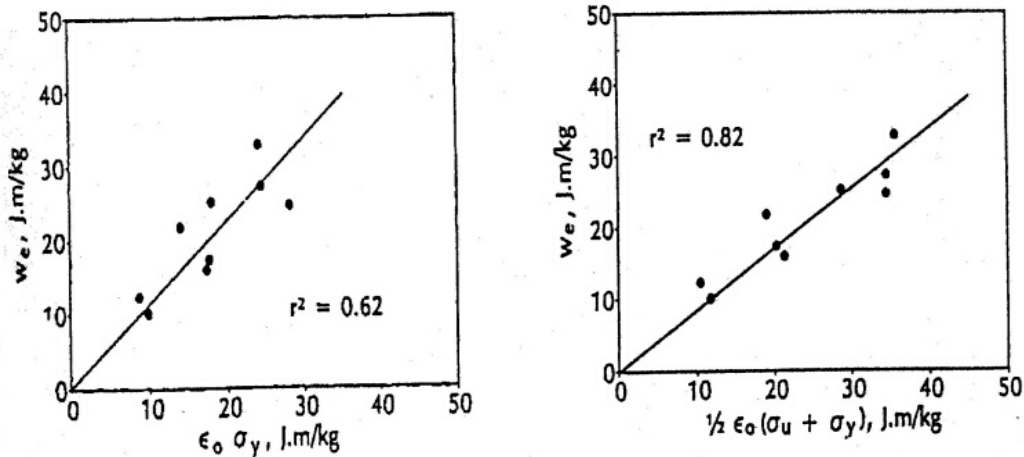


Figure 2.33 w_e against specific fracture energy calculated from equation (2.46). The left graph shows the specific fracture values calculated by substituting only the yield strength. The correlation is better when this value was replaced by $\frac{1}{2}(\sigma_u + \sigma_y)$ (see right graph) (Seth, 1993)

Therefore the average of the yield stress and the ultimate tensile stress (σ_u) was taken as the stress at the crack tip at the onset of crack propagation. The specific fracture energy or fracture toughness was then obtained using the equation

$$R = \epsilon_0 \sigma = \frac{1}{2} \epsilon_0 (\sigma_{ys} + \sigma_u) \quad 2.47$$

The plot of essential work of fracture (w_e) vs the fracture toughness estimated from equation (2.47) is shown in Figure 2.33. The yield stress of the specimens was obtained, from stress-strain curves of unnotched specimens, from the point at which the stress-strain curve deviated 0.2% from linearity.

2.9.6.3 Comparison of J-integral and EWF fracture toughness

Karenlampi *et al.*, (1998) compared the fracture energy obtained from the EWF technique and the J-integral method. The STFI J- integral method (Wellmar, Fellers et al. 1997) was used in the estimation of fracture toughness using the J-integral technique. The fracture energies obtained by the two methods were proportional to each other for brittle papers, but for tough ductile papers, the J-integral method gave a significantly lower value than the EWF method, as shown in Figure 2.34 (Wellmar, Fellers et al. 1997). Karenlampi *et al.* suggested that the most likely explanation for this discrepancy is that there are fundamental differences in the quantities measured in the two techniques as the J-integral technique estimates the critical value of the total energy release rate and the EWF method measures the energy release rate reaching the FPZ.

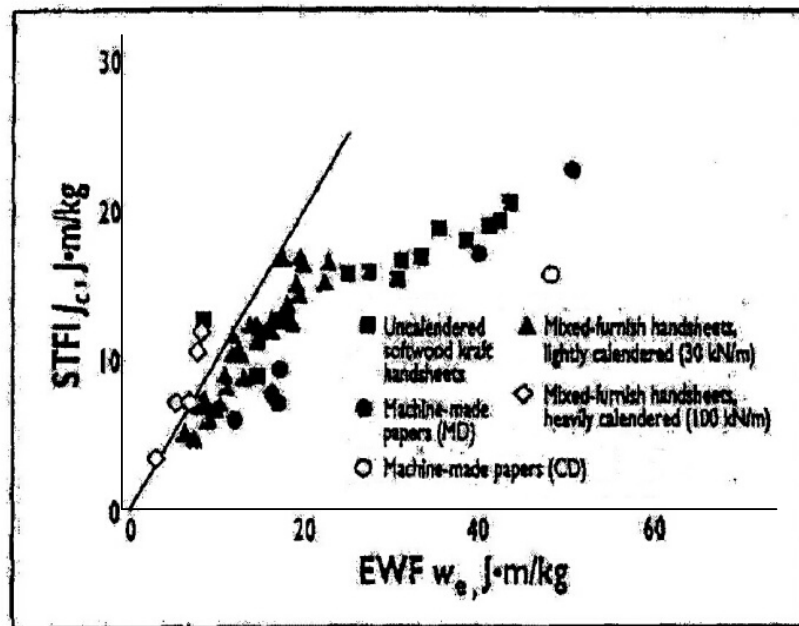
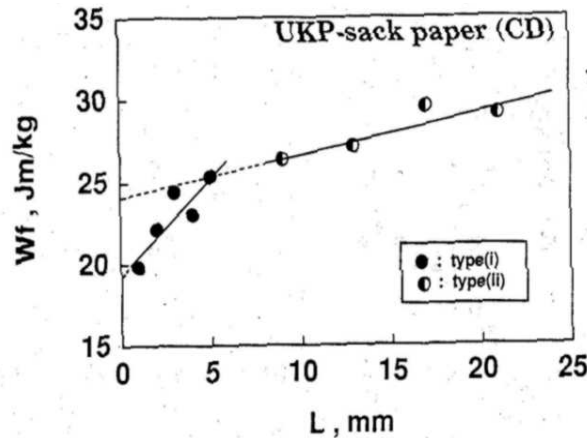


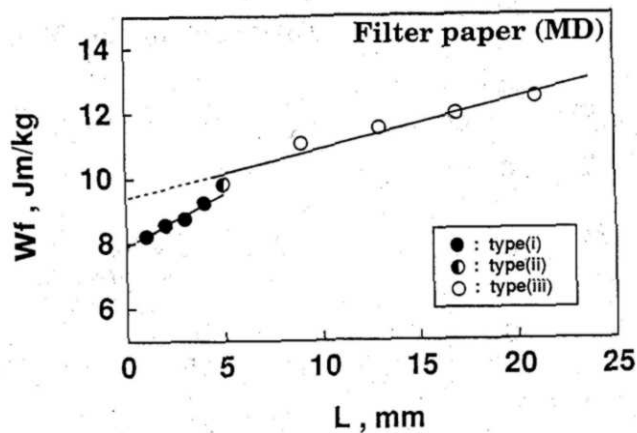
Figure 2.34 Comparison between EWF fracture toughness (w_e) and the J_c for different samples. Only the heavily calendered (brittle) papers show $J_c > w_e$ (Karenlampi, Cichoracki *et al.* 1998)

2.9.6.4 Examination of conditions in EWF using thermography

Employing infrared thermography, Tanaka *et al*, (1997; 1997; 2000) examined the validity of the EWF technique by observing the temperature distribution of a DENT paper specimen during EWF testing. They observed that the plastic deformation zone around the ligament appeared in three types. Type I was designated as a deformation field that extends through the whole ligament and eventually develops into a circular or oval zone before or at the maximum load point. Specimens with short ligaments were found to belong to this category.



(a)



(b)

Figure 2.35 Experimental plots of w_f against L for (a) sack paper and (b) filter paper (Tanaka and Yamauchi 2000)

Type II was identified as a deformation field that begins from the notch tips and then extends and overlaps to form a circular or oval zone after the maximum load point. A deformation field that appears from both notch tips and does not extend to form a single plastic zone before final failure was labeled as type III. For the tested samples, test

pieces with $L > 5\text{mm}$ were identified as belonging to type II or type III. They claimed that of the three types, only type I satisfies the original assumption of EWF technique, which is that “the ligament should completely yield before the crack propagation”. Figure 2.35 shows the experimental plots of w_f against ligament length for (a) sack paper (CD) and (b) filter paper (MD). The plots show the two different linear correlations of the data obtained from different types of deformation fields. Tanaka *et al* (2000) argued that only the specific essential work of fracture determined from a linear fit to data from tests showing type I deformation fields should be accurate. The EWF fracture toughness determined from measurements with type I deformation fields, will always be less than the fracture toughness measured if the sample has type II or III deformation fields.

This could be a major problem of using EWF technique, as type II and type III deformation fields also give a EWF plot with a straight line but with an inaccurate value. There is no easy way to identify whether the field is type I unless large numbers of samples with a full range of ligament lengths are tested to estimate, from the change in slope of the EWF plot, the ligament length ranges over which the different deformation fields develop.

Yu and Karenlampi (1997) investigated the elastic energy stored in DENT specimens at the instant of crack initiation and hence examined the stability of the crack growth. One of the conditions that should be satisfied for the EWF technique is stable crack growth (Seth, Robertson *et al.* 1993). They reported that stored elastic energy increased with specimen length and the crack length. Yu and Karenlampi (1997) stated that testing brittle materials with EWF method could be troublesome as the EWF method could overestimate the toughness if precautions are not taken to obtain a stable fracture. However, they found that the fracture toughness of tough and ductile specimens appeared to be independent of specimen dimensions, provided the sample length is not longer than its width.

2.10 Theoretical models on fracture toughness

There have been a few theoretical models proposed for the fracture toughness of paper (Shallhorn 1994; Ferahi, Kortschot *et al.* 1996; Niskanen, Karenlampi *et al.* 1996).

Ferahi *et al.*, (1996) proposed a novel model for fracture, using the anisotropic behavior of paper and a mixed mode fracture to predict paper web failures. From their model they concluded that: (a) anisotropic behavior of paper tends to produce crack propagation in a direction that does not correspond to the maximum stress intensity; (b) the fracture process in newsprint is of a mixed mode nature; (c) the breaks initiated by defects such as cracks are governed by a directional fracture toughness parameter; (d) the runnability of paper can be improved by reducing the anisotropy in mechanical properties and (e) a reduction in the thickness of shives is more effective in improving runnability than a reduction in the length of the shives. However so far there has been no independent experimental confirmation of these conclusions.

Shallhorn (1994) used a previous model proposed by Shallhorn and Karnis (1979) on paper failure to interpret the fracture resistance of some of the sheets prepared from mixtures of chemical and mechanical pulp. The model assumed that the fibres cross the crack path were bonded to a matrix of other fibres so that during tensile failure the fibres crossing the crack line are either pulled out of the matrix or break if the fibres were strongly bonded on either side of the crackline.

In this model, it was assumed that if the fibres are not well bonded to the matrix then all the fibres will pull out in failure, and the fracture resistance, R , is given by,

$$R = N\pi r\tau l^2/12 \quad \mathbf{2.48}$$

where N is the number of fibres per unit crack area, l is the fibre length, r is the fibre diameter and τ is the inter-fibre shear strength (ultimate shear stress at failure) due to inter-fibre bonding. For fibres with sufficiently large bonding (τ) (some fibres break), the fracture resistance is given by;

$$R = N\pi r^4\sigma^3 / (12l\tau^2) \quad \mathbf{2.49}$$

where σ is the fibre tensile strength.

Then the following relationships were obtained between the fracture resistance and paper tensile strength (T). For a weakly bonded sheet, where only fibre pull-out occurs,

$$R = lT / 6 \quad \mathbf{2.50}$$

and for a well bonded sheet (sufficiently large τ),

$$R = lT_o (1-T/T_o)^2 / 3 \quad \mathbf{2.51}$$

where $T_0 = N\pi r^2\sigma$ is the zero-span tensile strength.

Shallhorn (1994) reported that these expressions generally described the fracture-resistance-tensile curves shown for softwood pulp in previous work (Seth and Page 1975) where the fracture resistance increased initially with increasing tensile strength until it reached a maximum then began to decrease as tensile strength increased further. The maximum fracture resistance predicted from the model is given by,

$$R_{\max} = lT_0 / 12 \qquad \mathbf{2.52}$$

The maximum occurs at $T = T_0/2$ and fibre length is given by $l=6R / T$.

Based on the experimental results and the theoretical model Shallhorn reported that fracture resistance of sheets made from an unbeaten kraft pulp increased with increased bonding and he implied that fibre pull-out, rather than fibre breakage, is the dominant mechanism of energy dissipation for this pulp during fracture. He further related the increasing fracture resistance directly to the fibre length. However, one of the problems with this model is the use of in-plane tear strength as the fracture resistance. The relevancy of the use of in-plane tear strength to predict the fracture toughness or runnability of paper web was questioned due to its mixed mode type failure (Seth and Page 1975; Roisum 1990; Karenlampi, Retulainen *et al.* 1994; Niskanen, Karenlampi *et al.* 1996). In Chapter 7 of this thesis, this model will be compared with the results we obtained.

Starting from microscopic principles a model was proposed by Niskanen *et al.* (1996) for predicting fracture toughness of paper. In this model bond rupture and fibre fracture were treated as stochastic energy consuming processes. The model assumes that when a crack propagates across a paper specimen, any fibre crossing the fracture line should be released from one half of the sheet by either inter-fibre bonds breaking or the fibre breaking. If the release of fibre occurs due to inter-fibre bond breakage then the length of the fibre that has to come out of the matrix is at least x from the crack to the fibre end as shown in Figure 2.36. The average work required to release one fibre from bond failure and/or fibre failure is,

$$W_{\text{fibre}} = \left[w_f + \frac{(1-p_f)}{p_f} w_b \right] (1 - (1-p_f)^n) \quad 2.53$$

where w_b is the work needed to break a bond between two fibres, w_f is the average work needed to break a fibre (this includes the plastic deformations that occur within the fibre when it fails) and n ($= l_f/4l_s$ to $l_f/2l_s$) is the number of bonds to be broken to release the fibre when the fibre doesn't break. Here l_f and l_s are the fibre length and average distance from one bond to the other (on the top and bottom of the fibre) respectively. The probability

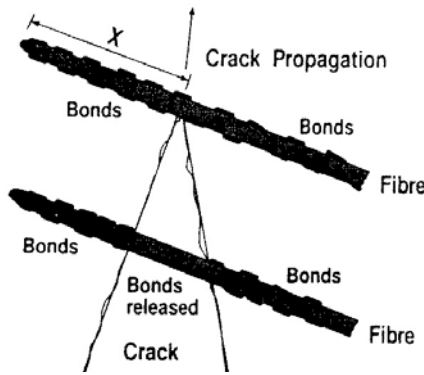


Figure 2.36 Two parallel fibres crossing the rupture line. The length of the fibre that has to be released is x in the case of a fibre pull-out (Niskanen, Karenlampi *et al.* 1996)

of fibre failure per bond rupture is taken as a constant and is given by p_f . The fracture toughness of the paper is then given by W_{fibre} x number of fibres crossing the rupture line per unit length. This number depends on the fibre coarseness, paper grammage and fibre orientation.

The fraction of fibre that rupture rather than pull out is given by;

$$N_{\text{fibre}} = 1 - (1-p_f)^n \quad 2.54$$

Then n was chosen arbitrarily such that $1/n = \lambda = 4l_s / l_f$, where $\lambda \rightarrow 0$ in the limit of short fibre segments. Therefore the work needed to release one fibre can be rewritten as,

$$W_{\text{fibre}} = N_{\text{fibre}} \left[w_f + \frac{(w_f l_f / 4) \lambda (1 - N_{\text{fibre}})^\lambda}{1 - (1 - N_{\text{fibre}})^\lambda} \right] \quad 2.55$$

Here $w_l = w_b/l_s$ and is the average bond-breaking energy per unit fibre length. Since the fibre segments in most ordinary paper grades are short, λ is small in any case. Hence the use of the limit $\lambda \rightarrow 0$ was justified. At this limit w_l should be independent of l_s and equation (2.55) can be rewritten as

$$W_{fibre} = N_{fibre} \left[w_f - \frac{(w_l l_f / 4)}{\ln(1 - N_{fibre})} \right] \quad 2.56$$

Niskanen *et al* then define $p'_f = p_f/\lambda$ and when $\lambda \rightarrow 0$, equation (2.54) becomes,

$$N_{fibre} = 1 - \exp(-p'_f) \quad 2.57$$

The total fibre length that has to be pulled out is given by,

$$L_{pull} = - \frac{N_{fibre} l_f / 4}{\ln(1 - N_{fibre})} \quad 2.58$$

According to this model, the factor $1/4$ in equation (2.58) is accurate only when the fibre length that is sticking out of the crack surface is accounted for. Now the fracture toughness per fibre (W_{fibre}) is given as,

$$W_{fibre} = N_{fibre} w_f + L_{pull} w_l \quad 2.59$$

In this model they predicted that toughness of the material (per fibre) should be proportional to fibre length and not the square of fibre length as predicted from Shallhorn's (1994) model. Experimental work to test the model was also carried out by Niskanen *et al*. For both lightly and heavily beaten pulps the toughness per fibre appears to be linear function of fibre length. However, when the paper toughness (J_c) was plotted against fibre length, then only the heavily beaten pulp exhibited a linear dependence on fibre length. In addition, when sheet toughness was extrapolated towards zero fibre length, then the x-axis (fibre length) intercept of the extrapolation was greater than 0.

2.10.1 Summary:

The models proposed on the fracture toughness of paper have certainly provided some assistance in understanding and predicting fracture toughness. However further evaluations of these models are required to confirm their ability to predict fracture toughness accurately. Again considering the complexity in the fracture behavior of a

heterogeneous material like paper, constructing a model to include all of the possible variables is not easy task. However, a more satisfactory empirical model in this area could give a better fundamental understanding of the factors affecting the fracture toughness of paper and therefore an improvement in the prediction of runnability of paper.

2.11 Concluding remarks

Significant advances have been made in the characterization of paper fracture toughness and improving web runnability. The developments have included the use of statistical methods as well as the development of non-linear fracture mechanics techniques. Even with these advances there is still a requirement for a more convenient technique that can accurately and rapidly characterize fracture toughness.